國立交通大學

生化工程研究所碩士班

論文口試委員會審定書

本校 生化工程研究所 碩士班 賴紹全 君

所提論文(中文) 阿黴素誘發心肌病小鼠之心臟組織中基質金屬蛋白酶與其組織抑制因子表現樣態的探討

(英文) Studying the Expression Profiles of Myocardial Matrix Metalloproteinases and Tissue Inhibitor of Metalloproteinases in the Mouse Hearts with Doxorubicin-Induced Cardiomyopathy

合於碩士資格水準、業經本委員會評審認可。

口試委員：吳介信 教授 吳介信 教授

吳希天 教授 吳希天 教授

楊昀良 教授 楊昀良 教授

廖光文 教授 廖光文 教授

指導教授：林志生 教授 林志生 教授

所長： 教授

中華民國 年 月 日

國 立 交 通 大 學

生 物 科 技 學 院

生 化 工 程 研 究 所

碩 士 論 文

阿黴素誘發心肌病小鼠之心臟組織中基質金屬蛋白酶與其組織抑制因子表現樣態的探討

Studying the Expression Profiles of Myocardial Matrix Metalloproteinases and Tissue Inhibitor of Metalloproteinases in the Mouse Hearts with Doxorubicin-Induced Cardiomyopathy

研 究 生：賴 紹 全

指導教授：林 志 生 博士

中 華 民 國 九 十 七 年 七 月

謝　　誌

我很慶幸在這兩年辛苦的研究生活中，是在一個充滿歡笑，和樂融融的實驗室中度過。如果以後我對外面環境的險惡無法適應，都是你們害的。首先，我要感謝**建龍**學長在我剛進這個實驗室的暑假，帶著我踏入這個領域的研究。學長在研究上的創造力、實驗中的“sense”以致於對data的解釋能力都是我所望塵莫及的。我從學長身上學到了很多，多到在暑假終了老師回國之後，忘記是什麼原因唸了我“有什麼師父就有什麼樣的徒弟”！不過我想這一定是我自己的問題，絕對與學長無關的；另一位心血管組的**俊旭**學長，在我跟著他學習cloning以及細胞實驗的同時，見識到了學長的嚴謹。不過更令我印象深刻的是學長溫文儒雅、好好先生的脾氣。記得有一次本人不小心毀了學長construct了三天三夜的成品，當下真是惶恐不已。所幸學長並未追究及記恨，真不愧是虔誠的天主教修行人；**証皓**，這位從中國醫來的學弟，可說是我的左右手幫了我不少的忙。沒有他幫我抓著小鼠節省下不少保定時間的話，我可能到現在還在跟小鼠玩更不用說畢業了；此外，我還要感謝**棠青**學長在重要的時候總可以提供他的車子幫了我很多的忙；以及我的三位同學：**聖壹、曜禎**及**宜貞**，在這大家一起奮鬥經歷的兩年中，相互的支持及砥勉（預祝你們博班與就業順利）；還有實驗室永遠的助理－**千雅**，有你實驗室財產才得以僅然有序，有你大家才不會錯過了吃飯的時間。對於其他不及被載的實驗室成員們，感謝你們平日的幫忙及照顧，我才得以完成此本論文並順利畢業。

當然，我最感謝的還是我的指導教授－**林志生老師**。老師早在我大學時期就已經是我的導師，可說照顧了我六年之久。我一直記得老師在我大一時的導生會談上對我的期許，令六年後今日的我不禁感到有些汗顏。老師對於研究上的指導，常常在觀念上給予我重要的啟發。在實驗的細微環節上，也總不吝惜地提出以往自己的實驗經驗給我學習參考。在此篇論文的寫作上，更是花了相當多的時間在幫我修改儘管老師已是如此地忙碌。在這兩年間老師對於我的指導以及包容，令我銘感五內，這已不是單單感謝一詞所可以道盡的了。

最後，我要非常感謝 **吳介信老師**、**吳希天老師**、**楊昀良老師**及**廖光文老師**能來擔任我的口試委員，因為老師們的高抬貴手及相當有價值的建議，讓我能在最後一刻，順利的取得學位。另外，還有在此研究中犧牲奉獻的動物們，沒有你們就沒有這篇論文，更遑論人類醫療的進步。當然，我也要感謝我的家人在背後默默的付出，沒有你們的支持也不會有今日的我。真的非常謝謝大家，為我做的一切，因為有你們，我才能如願取得學位。

阿黴素誘發心肌病小鼠之心臟組織中基質金屬蛋白酶與其組織抑制因子表現樣態的探討

研究生：賴紹全　　指導教授：林志生博士

國立交通大學
生物科技學院
生化工程研究所碩士班

中文摘要

心臟結構與功能上之失調是心臟衰竭（heart failure, HF）臨床上的表徵，其為常見之病症，以及造成死亡的普遍原因。異常之細胞外基質（extracellular matrix, ECM）重塑（remodeling）被認為在HF病程之結構性異常中扮演著重要的角色。基質金屬蛋白酶（matrix metalloproteinases, MMPs）是一類活性依賴於Zn^{2+}等金屬離子且參與降解ECM的蛋白酶家族，其與內源性的MMPs組織抑制因子（tissue inhibitor of metalloproteinases, TIMPs）精密調控著組織中ECM的代謝。許多證據顯示多種心血管疾病與MMPs和TIMPs間的表現失調相關。阿黴素(doxorubicin, Dox）廣泛使用於腫瘤之臨床治療，但其應用受到給予劑量累積可能導致的心臟毒性，以致引發心肌病而有所限制。據此，我們利用Dox誘發HF的小鼠動物模式來檢視此心肌病病程中MMPs及TIMPs的表現樣態。

在本研究中，C57BL/6J 小鼠每週以腹腔注射 4 mg/kg 劑量的 Dox 直到 20 mg/kg 的累積劑量。小鼠的左心室將分別在第一劑給藥之後的第 1, 3, 5, 9 及 12 週取出，以

用於 MMP-1、MMP-2、MMP-9 及 TIMPs 表現樣態之分析。根據心電圖與 HF 生物性指標分析，S-T 區間的增長與心臟組織利鈉激素 A（atrial natriuretic peptide）及利鈉激素 B（brain natriuretic peptide）的 mRNA 上升顯示出 Dox 心臟毒性的效應。於基因表現上，明膠酶（gelatinase）（包含 MMP-2 與 MMP-9）基因的表達在此疾病模式後期有下降的趨勢，然而膠原蛋白（collagen）與 TIMPs 的基因表現呈現穩定狀況。在蛋白質分析中顯示，雖然整體 MMP-1 的蛋白質表現量並沒有受到 Dox 處理的影響，但活化態的 MMP-1（act-MMP-1）隨著處理時間的延長有逐漸增加的現象。藉由膠內酶譜（in-gel zymography）分析，結果顯示 MMP-9 活性在第一週有上升的情形，其後隨著病程的延長，gelatinase 活性呈現下降，此現象與基因表現上的樣態趨勢類似。然而，與 gelatinase 活性的變化相反，TIMPs 的活性是隨著 HF 病程時間的延長而上升。

我們演示了 Dox 誘發之心肌病模式中小鼠左心室心肌內 MMPs 和 TIMPs 之時間相依性之變化。在本研究結果中可歸納出幾項值得注意的發現，此包含 MMP-1 活化的漸進增加、gelatinase 基因的表達下降、gelatinase 活性降低及 TIMPs 活性的上升。這些心臟組織中的 MMPs 及 TIMPs 變化樣態可助於釐清 Dox 誘發之心肌病中心臟結構重塑的機轉。

Studying the Expression Profiles of Myocardial Matrix Metalloproteinases and Tissue Inhibitor of Metalloproteinases in the Mouse Hearts with Doxorubicin-Induced Cardiomyopathy

Graduate Student: Shao-Chuan Lai Advisor: Chih-Sheng Lin Ph. D.

Institute of Biochemical Engineering

College of Biological Science and Technology

National Chiao Tung University

Abstract

Heart failure (HF), a common cause of morbidity and mortality, is a clinical syndrome characterized by structural and functional cardiac disorder. Abnormal metabolism of extracellular matrix (ECM) has been proposed to participate in structural remodeling during the progressive development of HF. ECM metabolism tissue is precisely modulated by matrix metalloproteinases (MMPs) and their native inhibitors, tissue inhibitor of metalloproteinases (TIMPs). MMPs constitute a family of extracellular zinc-dependent endopeptidases and can degrade essentially ECM components. Various evidences have shown that several cardiovascular diseases are associated with imbalance of MMPs and TIMPs. Doxorubicin (Dox) is widely used for clinical treatment of a variety of malignancy. Usefulness of Dox is limited, however, by its cardiotoxicity which may result in cardiomyopathy in a dose-dependent manner. Thus, we utilized Dox to induce HF and examined the expression profiles of MMPs and TIMPs during the process of chronic cardiomyopathy in a mouse model.

In this study, C57BL/6J mice were intraperitoneal injection with 4 mg/kg of Dox weekly until reaching the accumulated dosage of 20 mg/kg. The left ventricles (LV) of animals were

harvested at week 1, 3, 5, 9 and 12 after the first injection for examining the expression profiles of MMP-1, MMP-2, MMP-9 and TIMPs. According to the analyses of electrocardiogram and HF biomarker, increased S-T interval and up-expressed mRNA of atrial natriuretic peptide and brain natriuretic peptide indicated the effects of Dox cardiotoxicity. At transcriptional level, the transcripts of gelatinase (MMP-2 and MMP-9) were down-expressed but collagen and TIMPs expression were stable during the end stage of model. At protein expression level, total MMP-1 was not influenced by Dox treatment but active form of MMP-1 (act-MMP-1) was progressively increased over time. By in-gel zymography analysis, the increased MMP-9 activity was detected at first week and then gelatinase activity during end stage was reduced as similar as the gene expression profile. In contrast to gelatinase, the TIMPs activity was increased according to the measurement of reverse zymography.

In conclusion, we demonstrated a time-dependent alteration of MMPs and TIMPs in mouse LV with Dox-induced cardiomyopathy. Several notable findings were discovered including gradual increase of MMP-1 activation, reduction of mRNA and enzyme activity of gelatinase, and induction of TIMPs activity in the Dox-induced cardiomyopathy. These expression profiles of the myocardial MMPs and TIMPs may provide insight into the mechanism of cardiac remodeling in Dox-induced cardiomyopathy.

Content

List of Tables

List of Figures

I. *Literature reviews*

1-1. Heart failure and cardiac remodeling

Heart failure (HF), a condition that impairs the ability of the heart to pump a sufficient amount of blood through the body, is a common cause of morbidity and mortality, and the incidence is increasing because of the aging population (Mathew et al., 2004; Hunt, 2005). Following a specific cardiovascular stress, a cascade of compensatory structural events occurs within the myocardium and contributes to eventual left ventricular (LV) dysfunction and the manifestation of the heart failure syndrome (Spinale, 2007). The summation of both cellular and extracellular alterations, a process termed cardiac remodeling, is revealed clinically as changes in the size, shape, and function of the heart (Swynghedauw, 1999; Cohn et al., 2000; Leri et al., 2005). Histopathologically, it is characterized by a structural rearrangement of components of the normal chamber wall that involved cardiomyocyte hypertrophy, cardiac fibroblast proliferation, fibrosis, and cell death (Swynghedauw, 1999). Irrespective of its cause, this maladaptive remodeling contributes to diminished systolic performance, decreased compliance, and diastolic dysfunction in failing human heart (Brilla and Rupp, 1994).

1-2. ECM Remodeling and fibrosis

The myocardial extracellular matrix (ECM) is made up of fibrillar collagens network, basement membrane, proteoglycans, glycosamioglycans and contains a diverse array of bioactive signaling molecules (Janicki and Brower, 2002; Ito et al., 2005). The fibrillar collagen network ensures the structural integrity of the adjoining myocytes, provides the means by which myocyte shortening is translated into ventricular pump function, and is essential for maintaining alignment of the myofibrils within the myocytes through with a collagen-integrin-cytoskeletal myofibril relation (Janicki and Brower, 2002). Mechanical

stimuli such as stress or strain are likely transduced through the myocardial ECM to the cardiac myocyte, which in turn would directly affect myocyte growth (MacKenna et al., 2000; Borer et al., 2002). In addition to a fibrillar collagen network, the myocardial ECM contains a large reservoir of bioactive molecules that directly influence myocardial ECM synthesis and degradation (Chen et al., 2000; Cucoranu et al., 2005).

Fibrosis, which is a disproportionate accumulation of fibrillar collagen, is an integral feature of the remodeling characteristic of the failing heart (Kostin et al., 2000). Accumulation of type I collagen, the main fibrillar collagen found in cardiac fibrosis, stiffens the ventricles and impedes both contraction and relaxation (Sun and Weber, 2005; Zannad and Radauceanu, 2005). Fibrosis can also impair the electrical coupling of cardiomyocytes by separating myocytes with ECM proteins (Swynghedauw, 1999). Furthermore, fibrosis results in reduced capillary density and an increased oxygen diffusion distance that can lead to hypoxia of myocytes (Sabbah et al., 1995). Thus, it profoundly affectes myocyte metabolism and performance and ultimately alters ventricular function (Schnee and Hsueh, 2000; Manabe et al., 2002).

Fibrosis has been classified into two groups: reparative and reactive fibrosis. Reparative (replacement) fibrosis or scarring accompanies myocyte death. It is a result of a scarring process in which areas of necrosis heal after direct insults such as myocardial infarction (Whittaker, 1995). Reactive fibrosis appears as “interstitial” or “perivascular” fibrosis and does not directly associate with myocyte death. It may be a fibrogenic response of the myocardium to a variety of stimuli. In interstitial fibrosis, fibrillar collagen appears in intermuscular spaces (Kai et al., 2005). Perivascular firosis refers to the accumulation of collagen within the adventitia of intramyocardial coronary arteries and arterioles. Although there are a number of apparent differences between reparative and reactive fibrosis (e.g. cells involved and the time course of fibrotic change), many factors likely work in common to

control fibroblasts function (Kai et al., 2005).

Cardiac fibrosis is not only an increase in the concentration of matrix collagens but also changes in collagen type, organization and cross-links (Whittaker, 1995). Thus, despite the significant increase in collagen production, the replacement collagen is poorly cross-linked (Gunja-Smith et al., 1996). This compromises the supportive scaffolding leading to cell slippage, LV dilation and diminished diastolic compliance (Feldman et al., 2001). Various changes in the composition of collagen types and cross-links have been reported during the development of cardiac fibrosis in different animal models as well as in patients with heart failure (Li et al., 2000).

1-3. ECM remodeling and MMPs

The ECM is a dynamic structure with continuous changes in the amount and proportions of its structural proteins (Dollery et al., 1995). The integrity of ECM is maintained by a balance in the activity of matrix metalloproteinases (MMPs), a family of enzymes that degrade all the matrix components of the heart, and their tissue inhibitors, TIMPs. Thus, an increase in MMP activity may result in fibrillar collagen degradation, ECM remodeling, and progressive ventricular dilatation (Li et al., 2000). MMPs not only play a role in ECM degradation but also synthesis. The end results is often increased MMPs accompanied with increased fibrosis in HF, and decreased MMPs activity accompanied with decreased fibrosis (Heymans et al., 1999). MMPs may participate in the fibrosis and remodeling process through direct digestion of matrix components, and regulation of the formation of matrikines such as glycyl–histidyl–lysine, derived from several degraded ECM protein can stimulate new connective tissue forming (Maquart et al., 1988), and release of biologically active factors from the ECM (Taipale and Keski-Oja, 1997).

The expressions of ECM and MMPs change dynamically during the developmental process of heart failure (Moshal et al., 2005). **Table 1** summarizes the reported changes in MMPs and TIMPs profiles in dilated cardiomyopathy (DCM) in human. These studies indicate that although maladaptive remodeling in cardiac disease is generally associated with enhanced MMP and reduced TIMP activities, this pattern is not held universally and varies with the etiology, different stages of the disease or the effects of HF treatment (Kassiri and Khokha, 2005). In addition, genetic manipulation of different MMPs or TIMPs in animal models has provided insights into their roles in cardiovascular development and in progression of cardiac disease. **Table 2** summarizes several results from MMPs and TIMPs transgenic studies.

1-4. MMPs : structures and functions

MMPs is a family of extracellular zinc-dependent neutral endopeptidases (Lombard et al., 2005), capable of degrading essentially all ECM components including fibrillar and non-fibrillar collagens, fibronectin, laminin and basement membrane glycoproteins (Fedarko et al., 2004). MMPs not only play an important role in ECM remodeling in physiologic situations, such as embryonal development, tissue regeneration, and wound repair, also in pathological conditions including rheumatoid arthritis, osteoarthritis, atherosclerotic plaque rupture, tissue ulceration, and in cancer cell invasion and metastasis (Roeb and Matern, 2001; Jones et al., 2003).

MMPs are generally divided into six groups, interstitial collagenases (MMP-1, -8 and -13), stromelysins (MMP-3, -10, -11 and -12), matrilysins (MMP-7 and MMP-26), gelatinases (MMP-2 and MMP-9), membrane-type MMPs (MMP-14, -15, -16, -17, -24 and -25) and others (Hijova, 2005). Although MMPs are subclassified based on their ability to degrade

various proteins of the ECM, they also play other important roles such as the activation of cell surface receptors and chemokines (Stefanidakis and Koivunen, 2006). In addition, MMP-2 has proteolytic activity to specific targets within the cell to cause acute, reversible contractile dysfunction in cardiac disease (Schulz, 2007). Classification and nomenclature of all the types of MMPs were listed in **Table 3.** The basic structures of MMPs can be approximately divided into three structurally well-preserved domain motifs, including a catalytic domain, an N-terminal domain and a C-terminal domain. Zinc-dependent catalytic domain of MMPs is similar with subtle structural differences among the substrate specific groups (Nagase and Woessner, 1999). The N-terminal domain (propeptide domain) contains a unique PRCG(V/N)PD sequence in which the cysteine residue interacts with the catalytic zinc atom in the active site, prohibiting activity of the MMPs. Thus, the interaction has to be disrupted to "open" the cysteine switch in the process of MMPs activation (van Wart and Birkedal-Hansen, 1990), which is a critical step that leads to ECM breakdown (Carmeli et al., 2004). The C-terminal hemopexin domain of metalloproteinases has a four-bladed propeller structure and contributes to substrate specificity (Wallon and Overall, 1997). In membrane-type MMPs, the hemopexin domain contains a transmembrane domain for anchoring the protein in the membrane; besides, the hemopexin domain in MMP-2 also has a function in the activation of the enzyme (Morgunova et al., 1999; Overall et al., 1999). The regulation of MMPs occurs at many levels, including transcription (the major one), post-transcriptional modulation of mRNA stability, secretion, localization, zymogen (proenzyme) activation and inhibition of activity by natural inhibitors of MMPs, tissue inhibitor of metalloproteinases (TIMPs).

1-4-1. Collagenase-1 (MMP-1)

MMP-1 was first purified from the tail of tadpole, the collagenolytic activity is required

to digest the collagen of the tail during amphibian metamorphosis (Gross and Lapiere, 1962). Human MMP-1 cDNA clone and the sequence were obtained from adult skin fibroblasts (Goldberg et al., 1986). Human MMP-1 is produced as two differently glycosylated proenzymes, a major 52 kDa and a minor 57 kDa form. Activation of these two latent forms generates two active proteinases 42 kDa and 47 kDa in size, respectively (Wilhelm et al., 1986). It was considered that MMP-1 was deficient in rodent until two closely related mouse counterparts to human MMP-1 were cloned: Mcol-A and Mcol-B. The Mcol-A and Mcol-B are expressed during embryo implantation, but only Mcol-A is able to cleave fibrillar collagens (Balbin et al., 2001).

1-4-2. Gelatinase A (MMP-2)

In 1978, Sellers et al. were first to separate a gelatinase activity from collagenase and stromelysin in the culture medium from rabbit bone (Sellers et al., 1978). A similar enzyme, acting on basement membrane type IV collagen was reported by Liotta et al. (1979) in the following year. Gelatinase was purified from human skin, mouse tumor cells, rabbit bone, and human gingival. The completed sequence of the human MMP-2 except for the signal peptide was reported by Collier et al. (2001). Gelainase A has a triple repeat of fibronectin type I domains inserted in the catalytic domain; this domain participates in binding to the gelatin substrates of the enzyme (Libson et al., 1995; Lee et al., 1997). MMP-2 is ubiquitously expressed in the cells which comprise the heart and is found in normal cardiomyocytes, as well as in endothelium, vascular smooth muscle cells and fibroblasts (Coker et al., 1999).

1-4-3. Gelatinase B (MMP-9)

In 1972, Harrwas and Krane detected a gelatinase activity in rheumatoid synovial fluid.

Sopata et al. described a gelatinase from human polymorphonuclear leukocytes (Sopata and Wize, 1979). Rabbit macrophages produce a very similar enzyme which is able to digest type V collagen (Horwitz et al., 1977). The neutrophil collagenase and gelatinase were resolved in 1980 (Murphy et al., 1980). Purification of MMP-9 protein was achieved in 1983 and sequencing of the cDNA was completed in 1989. An interesting phenomenon, still not fully understood, is the binding of TIMP-1 to proMMP-9 to form a complex (Sakyo et al., 1983; Stetler-Stevenson et al., 1989). Human neutrophil MMP-9 commonly occurs as a complex with lipocalin (Fernandez et al., 2005). A series of papers concerned a 95 kDa protein in plasma that binds to gelatin culminated in the identification of this protein as MMP-9 (Makowski and Ramsby, 1998).

1-5. TIMPs: structures and functions

The family of TIMPs presently numbers four distinct gene products that are specific inhibitors of the MMPs through binding in a 1:1 stoichiometry reversibly (Cook et al., 1994; Okada et al., 1994; Silbiger et al., 1994; Greene et al., 1996). These secreted proteins are thought to regulate MMPs activity during tisssue remodeling (Baker et al., 2002). All four mammalian TIMPs have many basic similarities, but they exhibit distinctively structural features, biochemical properties and expression patterns (**Table 4**). This suggests that each TIMP has specific roles in vivo. The local balance between MMPs and TIMPs is believed to play a major role in ECM remodeling during process of diseases such as cancer and arthritis (Anand-Apte et al., 1996). The TIMPs have molecular weights of ~20 to 30 kDa and are variably glycosylated (Baker et al., 2002). They have six disulphide bonds and comprise a three-loop N-terminal domain and an interacting three-loop C-subdomain. Most of the biological functions of these proteins discovere thus far are attributable sequences within the N-terminal domain, although the C-subdomain mediated interaction with the catalytic

domains of some MMPs (Li et al., 1999) and with the hemopexin domains of MMP-2 and MMP-9 (Brew et al., 2000). The TIMPs are secreted proteins, but may be found at the cell surface in association with membrane-bound proteins; for example, TIMP-2, TIMP-3 and TIMP-4 can bind MMP-14, a membrane-type (MT) MMP. All four TIMPs inhibit active forms of all MMPs studies to date, their binding constants being in the low picomolar range, although TIMP-1 is a poor inhibitor of MMP-19 and a number of the MT-MMPs (Baker et al., 2002).

1-6. Doxorubicin and cardiotocixity

Doxorubicin (Dox; adriamycin) is one of the original anthracyclines isolated in the early 1960s from the pigment-producing bacterium *Streptomyces peucetius* (Takemura and Fujiwara, 2007). Dox is one of the most widely used antitumor drugs. It is effective against a wide spectrum of cancers including acute leukemia, Hodgkin's and non-Hodgkin's lymphoma, and breast cancer (Weiss, 1992; Singal and Iliskovic, 1998). The mechanisms of antitumor that have been suggested include: (1) intercalation into DNA, leading to inhibition of synthesis of macromolecules; (2) generation of reactive oxygen species (ROS), leading to DNA damage or lipid peroxidation; (3) DNA binding and alkylation; (4) DNA cross-linking; (5) interference with DNA unwinding or DNA strand separation and helicase activity; (6) direct membrane effects; (7) initiation of DNA damage via inhibition of topoisomerase II; and (8) induction of apoptosis in response to topoisomerase II inhibition (Gewirtz, 1999; Minotti et al., 2004). Despite the usefulness, the side effects of Dox can cause dilated cardiomyopathy in a dose-dependent manner. The sharp increase in the incidence of cardiomyopathy at cumulative doses above 550 to 600 mg of Dox per square meter of body surface area has formed the basis to set an empirical dose limit of 500 mg/m^2 (Minotti et al., 2004). Progressive ventricular dysfunction and congestive heart failure may occur after the patients

even have stopped Dox treatments (Singal et al., 1987). The mechanism of the cardiotoxicity remains unclear, but it is likely to be distinct from the mechanism of antitumor. Most studies support the view that an increase in oxidative stress, evidenced increases in the levels of ROS (Kalyanaraman et al., 1980; Doroshow, 1983), and lipid peroxidation (Singal et al., 1985; Singal et al., 1987), along with reductions in the levels of antioxidants and sulfhydryl groups (Odom et al., 1992), play a key role in the pathogenesis of Dox-induced cardiomyopathy.

1-7. Monitor of cardiotoxicity

1-7-1. Electrocardiography

Electrocardiography (ECG) is a widely used and inexpensive technique. It is also considered useful in the identification of cardiotoxic effects induced by Dox. The changes of ECG on patients treated with Dox may occur including reduction in the voltage of the QRS-wave, T-wave flattening (Huang et al., 2004) and Q-T interval extension (Nousiainen et al., 1999). Although ECG is not a functional parameter, several studies have described the ECG changes in the animals upon administration of anthracyclines. The increased S-T interval was monitored by telemetric ECG system in non-anesthetic mice with administration of Dox (van Acker et al., 1996; Fisher et al., 2005). The widening of the S-T interval, which stands for the prolongation of the repolarization phase, may be explained by the prolongation of the action potential (van Acker et al., 1996). The action potential has been prolonged in Purkinje fibers after incubation with Dox (le Marec et al., 1986). On the other hand, Dox induced a lengthening of the P-R (Puri et al., 2005), Q-T interval (Sacco et al., 2001) in rats and a decreased amplitude of R-wave in canines were reported (de Souza and Camacho, 2006).

1-7-2. Natriuretic peptides

There are three major natriuretic peptides, atrial natriuretic peptide (ANP), brain natriuretic peptide (B-type NP, BNP), and C-type natriuretic peptide. Natriuretic peptides belong to a family of structurally related peptides and share the similar features of bioactivity. ANP, which was isolated from right atrium extracts in 1981 (de Bold et al., 1981), is preferentially synthesized and secreted from atria under physiological conditions (de Bold, 1985). BNP is synthesized in both atria and ventricles, but is predominantly released from the latter (Mukoyama et al., 1991). However, ANP and BNP can be synthesized in either chamber under pathologic conditions (Yasue et al., 1994), which play roles as hormones to act in various tissues in body and induce vasodilation, natriuresis, and diuresis to protect the cardiovascular system from overload (Nakao et al., 1992). The plasma levels of natriuretic peptides have been shown to be increased in patients with CHF (Wei et al., 1993), besides, the amount of natriuretic peptides highly correlating to cardiovascular diseases as a potential marker have been reported (Daniels and Maisel, 2007).

In Dox-induced cardiomyopathy, the measurement of plasma ANP (Bauch et al., 1992; Hayakawa et al., 2001), N-terminal proANP (Tikanoja et al., 1998), BNP (Pinarli et al., 2005) and N-terminal proBNP (Soker and Kervancioglu, 2005) during anthracycline treatment in clinical studies were reported, suggest that ANP and BNP are also useful makers of LV dysfunction in patients undergoing anthracycline therapy (Bryant et al., 2007). In the experiment of animal model, the increase of ANP mRNA in the hearts of Dox-treated dog, rat (Rahman et al., 2001) and rabbit (Boucek et al., 1999) were demonstrated. In addition, the Dox-treated neonatal piglets revealed increased BNP mRNA levels in LV and RV (Torrado et al., 2003), and the plasma level of BNP but not ANP was significantly increased in Dox-treated rats (Koh et al., 2004). Nevertheless, the plasma BNP was not augmented in a canine model (Alves de Souza and Camacho, 2006).

II. *Materials and Methods*

2-1. Animals and Experimental model

8- to 12-wk-old male C57BL/6J mice were purchased from National Laboratory Animal Center (NLAC) Taipei, Taiwan. The animals were maintained on a standard laboratory diet and tap water, and exposed to a 12/12 h light–dark cycle. Ambient temperature and humidity during the study were maintained at about 22℃ and 65%, respectively. The animals were allowed to adapt to the laboratory housing conditions for at least 1 week before starting the experiment. The mouse model of Dox-induced cardiotoxicity was referred to previous studies (Delgado et al., 2004; Fisher et al., 2005). The animals were randomized into 1 of 5 groups and the heart of animals were isolated at week 1, 3, 5, 9, and 12 after the first injection; besides, each of the groups was subdivided into Dox administration and sham control groups (**Figure 1**). In the Dox group, the mice were administered with 4 mg/kg i.p. of Dox hydrochloride weekly for five weeks to reach the accumulated dosage of 20 mg/kg. Immediately before each infusion, lyophilized Dox hydrochloride was reconstituted by the addition of sterile saline (0.9% NaCl) solution to create a solution with a concentration of 1 mg/mL of Dox. The mice in sham control group received an equivalent volume of saline in place of Dox. All of the animals were observed daily and weighted once a week to record the physical condition. The experimental protocol conformed to the Guide for the Care and Use of Laboratory Animals (NIH Publication No. 85-23, revised 1996) and was approved by the animal welfare committees of the National Chiao Tung University.

2-2. Electrocardiography

Before sacrifice, animals were anesthetized with i.m. injection containing a combination of 50 mg/kg of Zoletil 50® (Virbac, Carros, France) and 15 mg/kg of Rompun® (Bayer,

Leverkusen, Germany). Lead II ECG was introduced by insertion of negative lead at the right shoulder and the positive lead toward the lower left chest. The electrodes were connected to an ECG module Biopac MP150 (Biopac Systems, Goleta, CA, USA), and data were recorded at 2000 Hz for 5 min per animal. The resulting ECG was analyzed by using acqknowledge software (Biopac Systems).

2-3. Tissue sampling and processing

The mice were sacrificed after 1, 3, 5, 9 and 12 weeks following the first injection with Dox or vehicle. After recording the ECG signal, the chest was opened and the heart was perfused with 20 mL ice-cold PBS at the flow speed of 4 mL/min. The remaining buffer was carefully eliminated before the heart was weighted, then the left ventricles were excised from the isolated hearts and tissue samples were stored at -80℃ until analysis. For pathological examination, the tissues were immersed in 4% paraformaldehyde for 24 hrs then dehydrated and embedded in paraffin wax. Tissue sections were processed by Haematoxylin & Eosin (HE) stain.

2-4. RNA isolation

Total cellular RNA of the left ventricles was extracted as recommended by the manufacturer of TRIzol™ (GIBCO BRL, Rockville, MD, USA). Briefly, the TRIzol method consists of the addition of 1 mL of the TRIzol reagent to each homogenized tissue (about 100 mg). The mixture was vigorously agitated for 30 sec and incubated at room temperature for 5 min. After this procedure, 200 μL chloroform was added to the tube, and the solution was centrifuged at 12,000 × *g* for 15 min. The aqueous phase was transferred to a clean tube, precipitated with 500 μL isopropyl alcohol, and centrifuged at 12,000 × *g* for 15 min. The

resulting RNA pellet was then washed with 1 mL of 75% cold ethanol and centrifuged at 7,500 × *g* at 4℃ for 5 min. The pellet was dried at room temperature, resuspended in 20 μL of diethylpyrocarbonate-treated water, and stored at −80℃. RNA was quantified by measuring absorbance at 260 nm and 280 nm and electrophoresed on a 1% denaturing agarose gel. The integrity and relative amounts of RNA were evaluated using ultraviolet visualization of ethidium bromide-stained RNA.

2-5. Reverse transcription-polymerase chain reaction

For cDNA synthesis, 3 μg RNA was supplemented in a total reaction volume of 20 μL with 1× reverse trascriptase (RT) buffer, 1 mM dNTPs, 2.5 μM oligo-dT (Toyobo, Osaka, Japan), 20 U RNase inhibitor (Toyobo), and 100 U ReverTra Ace® (Toyobo). After incubation for 50 min at 42℃, the mixture was incubated for 5 min at 99℃ to denature the products. The mixture was then chilled on ice. PCR primers for RT-PCR analysis were shown in **Table 5**. PCR reactions contained 4 μL cDNA, 2 μL each primer (10 μM), 5 μL 10 × PCR buffer, 2 μL 10 mM dNTP, 1 μL of 5 U/μL Taq polymerase (Violet Bioscience, Hsinchu, Taiwan) and 34 μL distilled water in a total volume of 50 μL. General thermal cycler (MiniCycler™; MJ Research, Waltham, MA, USA) conditions were as follows: 1 cycle of 5 min at 94℃, 24~38 cycles of denaturation at 94℃ for 30~60 sec, annealing at 55~60℃ for 30~60 sec, and elongation at 72℃ for 30~60 sec, and 1 cycle of 15 min at 72℃. The resulting PCR products were visualized on 2% agarose gels stained with SYBR Safe™ (Invitrogen, Carlsbad, CA, USA). The stained image was recorded by an image analyzer (DGIS-8 Digital Gel Image System; Topbio, Czech), and the band intensity was quantified using densitometric analysis by Scion image™ (National Institutes of Health, Bethesda, MD, USA). The relative mRNA expression of the collagen, ANP, BNP, and TIMPs were calculated as ratios to glyceraldehyde-3-phophate dehydrogenase (GAPDH) expression.

2-6. Quantitative real-time PCR

SYBR Green quantitative real-time reverse transcription-PCR (RT-PCR) was performed to detect the mRNA expression level of genes MMP-2, MMP-9 and GAPDH (as an internal control). The specific forward and reverse primers were designed with Primer Express software (Applied Biosystems, Foster, CA, USA) (**Table 5**). For each selected gene, the primer sets were tested for quality and efficiency to ensure optimal amplification of the samples. Real-time RT-PCR was performed at 1, 1/4, 1/16, 1/64, 1/128, and 1/512 dilution of the synthetic cDNAs from RT-PCR to define relative fold changes and optimal range. Real-time RT-PCR reaction contained 12.5 μL SYBR Green PCR master mix (Applied Biosystems), 400 nM forward primer, 400 nM reverse primer, 6 μL cDNA, and distilled water into a total 25 μL volume. All PCR reactions were carried out in triplicate with the following conditions: 2 min at 50℃, 12 min at 95℃, followed by 40 cycles of 15 sec at 95℃, and 1 min at 60℃, in an optical 8-tubes strip (Applied Biosystems) in the ABI 7000 Sequence Detection System (Applied Biosystems). A PCR reaction without cDNA was performed as a template-free negative control. According to the instructions of Applied Biosystems, the expression of each gene was quantified as ΔC_t (C_t of target gene − C_t of internal control gene) using GAPDH as the control and applying the formula $2^{-\Delta\Delta Ct}$ to calculate the relative fold changes (Livak and Schmittgen, 2001).

2-7. Protein extraction and electrophoresis

The frozen left ventricular tissues of mice were homogenized in ice-cold lysis buffer (by a ratio of volume:mass = 5:1) containing 50 mM Tris-HCl (PH 7.5), 150 mM NaCl, 10 mM $CaCl_2$, 0.02% NaN_3, 0.5 mM PMSF, 5% glycerol and 1% (v/v) Triton X-100. The

homogenates were then centrifuged at 12,000 × *g* at 4℃ for 30 min, and the supernatants were collected for sodium dodecyl sulfate-polyacrylamide gel electrophoresis (SDS-PAGE). Protein concentration was determined by the Bio-Rad protein assay kit (Bio-Rad, Hercules, CA, USA) with bovine serum albumin as a standard. Equal amounts of proteins (20 μg/lane) were separated on 10% polyacrylamide gels by SDS-PAGE.

2-8. Gelatin zymography

Zymography was performed by using gelatin-containing gels as described previously (Stawowy et al., 2004). Briefly, 20 μg of non-reduced tissue homogenates were mixed with zymography sample buffer, composed of 0.5 M Tris-HCl, pH 6.8, glycerol, 10% (w/v) SDS, and 0.1% bromophenol blue without reductant (mercaptoethanol or dithiothreitol), and stood for 10 min at room temperature, then loaded on each lane of an 10% SDS-polyacrylamide gel containing 0.1 mg/mL gelatin (Sigma, St. Louis, MO, USA), the stacking gel contained 5% acrylamide mix in 1.5 M Tris, pH 6.8. Following electrophoresis, the gel was washed twice for 30 min in zymogram renaturing buffer (2.5% Triton X-100) with gentle agitation at room temperature to remove SDS, then incubated at 37℃ for 24~48 hrs in developing buffer (50 mM Tris-HCl, pH 7.4, 200 mM NaCl, 5 mM $CaCl_2$). After coomassie brilliant blue (0.125% Coomassie Brilliant Blue R250, 50% (v/v) methanol, 10% (v/v) acetic acid) staining prior to destain with destain buffer (25% (v/v) methanol, 7.5% (v/v) acetic acid in ddH_2O), gelatinolytic activities were identified as clear zones against a blue background. Molecular weights of gelatinolytic bands were estimated by the positive control and protein marker. Gelatinase activities in the gel slabs were quantified using Scion image™ which quantifies both the surface and the intensity of lysis bands after scanning the gels.

2-9. Reverse gelatin zymography

Inhibitory activity of TIMPs was analyzed by reverse zymography as described previously (Oliver et al., 1997) with a slight modification. SDS-12% polyacrylamide gel was prepared with 1 mg/mL gelatin and 0.2 μg human MMP-2 control (cat. no. cc071; Chemicon, Temecula, CA, USA) in 10 mL running gel solution. It was overlaid with 5% stacking gel. Samples were mixed with equal volume of 2 × zymography sample buffer, and let the mixture stand for 10 min at room temperature. Applied samples (10 μg total protein/lane) and ran the gel with 1X Tris-glycine SDS running buffer (0.038 mM Tris base, 0.12 mM glycine, and 0.003 mM SDS) according to the standard running condition. After electrophoresis, gel was removed from the glass plate and incubated twice on a rotary shaker for 30 min in 2.5% Triton X-100. The Triton X-100 solution was decanted and replaced with 50 mL of developing buffer and the gel was incubated at 37℃ for 48 hrs. In the gel, protein bands from TIMPs were evident as darkly stained bands against a clear background. Dried gel was scanned as described above and quantified using Scion image™.

2-10. Western blot assay

Protein extracts of the left ventricular tissues separated by SDS-PAGE were electrophoretically transferred to PVDF membranes (Perkin Elmer Life Sciences, Inc., Boston, MA, USA) by semi-dry electroblotting (Hoefer^{TM}; Amersham Biosciences, Uppsala, Sweden). Briefly, nonspecific binding sites were blocked by incubating membranes in 5% non-fat milk of PBST (PBS with 0.1% Tween-20) for an hour and the membranes were incubated at 4℃ overnight with antibody against MMP-1 (1:3000 dilution of anti-MMP-1 mouse mAb, cat. no. IM35; Calbiochem, Little Chalfont, UK) and GAPDH (1:2000 dilution of anti-GAPDH goat pAb, cat. no. sc20357; Santa Cruz, Santa Cruz city, CA, USA) as internal control. The probed

blots were washed several times with PBST. Antibody binding of incubated horseradish peroxidase-conjugated donkey anti-goat IgG (1:2500 dilution, cat. no. sc2020; Santa Cruz) and horseradish peroxidase-conjugated **g**oat anti-mouse IgG **(**1:2500 dilution, cat. no. sc2005; Santa Cruz) in a condition of 4℃ for 4 hrs were visualized by Enhanced Luminol Chemiluminescence (ECL) Reagent (NEN, Boston, MA, USA) and by exposing the membranes to X-Ray film (Super Rx Medical X-Ray Film; Fujifilm, Kanagawa, Japan). The bands were detected at the expected size. The band intensity was quantified using densitometric analysis by imaging software Scion image™. The amount of MMP-1 was expressed relative to the amount of GAPDH in respective samples.

2-11. Statistical analysis

All data were expressed as mean ± standard deviation (SD). The difference between sham control and Dox groups was evaluated with the Student's t test. Statistical significance was considered if $P < 0.05$.

III. *Results*

3-1. Physiological examinations

During the Dox treatment, body weight of animals dropped to a mean weight loss of 8.4 ± 3.9% at week 4 and ultimately dropped to 11.4 ± 3.1% at week 12. In contrast, the sham control group gained a 20% increase in body weight during 12 weeks feeding and reached to a limit about 30 g. The significant differences ($P < 0.01$) between the groups and in comparison with the beginning were observed initially at week 2 and week 4, respectively (**Figure 2**). Furthermore, Dox treatment significantly decreased the ventricle weight and the ventricle weight/tail length ratio beginning from week 3 and further declined in the process (**Table 6**). The mortality of Dox-treated group was approximately 30% during 12 weeks. These mice died during week 5 to 12 primarily, even though Dox was not given to these mice during this time period.

3-2. Cardiotoxicity

Lead II electrocardiogram was introduced to monitor Dox-induced cardiotoxicity in this study according to the previous reports (van Acker et al., 1996). In contrast to ECG recordings in humans, the ECG does not contain an S-T segment in mice. The T-wave immediately follows the QRS complex; thus, no S-T segment can be found (**Figure 3B**). The prolongation of the S-T interval in Dox-treated mice is secondary to an increase in action potential duration. The ST interval in the Dox-treated group increased from 24.2 ± 2.0 msec at week 1 to 35.0 ± 0.2 msec at week 12. The differences relative to sham control group were significant ($P < 0.01$) beginning from week 5 (**Figure 3A**).

Besides the electrophysiological tests, natriuretic peptides which were previously used as

biomarker of heart failure in several Dox-induced cardiomyopathy animal models were surveyed in this study (Rahman et al., 2001; Torrado et al., 2003). The mRNA levels for ANP and BNP from the LV tissue were increased 4.0 ± 1.8 fold ($P < 0.01$) and 1.6 ± 0.3 fold ($P < 0.05$) compared with control at week 12, respectively (**Figure 4**). The expression of GAPDH mRNA was used as internal control.

3-3. Histological examinations

The histological differences between control and Dox-treated mice were shown in Figure 5. Hearts were examined at week 12 with use of hematoxylin and eosin staining. The ventricular sections demonstrated normal tissues in control mice (**Figure 5A**), whereas vacuolisation of cardiomyocytes existed in the Dox-treated mice (**Figure 5B**).

3-4. Expression of collagen type I and type III

We were interested in measuring the level of collagen type I and III in the tissue, which were predominant components of ECM. The transcript of collagen type I and III in the LV tissues were determined by semiquantitative RT-PCR (**Figure 6A**), and the expression of GAPDH mRNA was used as internal control. The expression level was presented as fold relative to control at each time point. After analysis, the statistical result showed no difference on mRNA expression level of collagen type I and III along the course (**Figure 6B and 6C**).

3-5. MMP-1: opposite trends of changes in latent and active form

Two major bands (57 kDa glycosylated latent proMMP-1 and 47 kDa active MMP-1) were detected on membrane by Western immunoblotting (**Figure 7A**). Comparing with

control, pro-MMP-1 in LV from Dox-treated mice increased 2.3 ± 0.7 fold ($P < 0.01$) at first week but trended down during the following stage. Except the first week, the amount of pro-MMP-1 in treated group was less than time-matched control mice with statistic significance, even decreased about 5-fold in the end point (**Figure 7B**). In contrast, the active form of MMP-1 had a notable tendency of increase in the process. The active MMP-1 increased significantly 2.6 ± 0.6 fold ($P < 0.01$) initially at week 5 and further ascended to 4.7 ± 0.7 fold ($P < 0.01$) at week 12 (**Figure 7C**). Collectively, an interesting pattern of the opposite trend of changes in latent and active form was illustrated in **Figure 7D**. Moreover, sum of these two forms was calculated as total MMP-1 protein roughly. Besides a decrease at week 3, there was no difference between two groups on total MMP-1 protein level (**Figure 7E**).

3-6. Decreased activity of MMP-2 and MMP-9

The LV tissue isolated from hearts with Dox-treated and control mice were used to detect the enzyme activity of two gelatinases, MMP-2 and MMP-9, by zymographic analysis (**Figure 8A**). As shown in **Figure 8C**, the 92 kDa pro-MMP-9 activity increased significantly by approximately 2 fold ($P < 0.05$) in the Dox-treated mice compared with control at first week but showed 2 fold decrease at week 12 ($P < 0.01$). The 68 kDa activation intermediate of MMP-2 displayed a similar pattern with pro-MMP-9 at the end stage; However, at week 12 MMP-2 only decrease about 1.5 fold ($P < 0.05$) (**Figure 8B**). In addition, a minor band on 72 kDa known as latent form MMP-2 showed no alteration in the whole process.

3-7. Decreased mRNA expression of MMP-2 and MMP-9

According to the results of zymographic assay, the down-regulated gelatinases activity

was observed in the LV of Dox–treated mice. Further, we measured the MMP-2 and MMP-9 mRNA levels by quantitative real-time PCR. The expression of GAPDH mRNA was used as internal control and the mRNA expression level were presented as fold related to control at each time point. The relative mRNA level of MMP-2 in the Dox group decreased 1.7 ± 0.2 fold and 1.6 ± 0.2 fold at week 9 and 12, respectively (Both $P < 0.01$) (**Figure 9A**). Similarly, the relative mRNA level of MMP-9 decreased 1.6 ± 0.2 fold and 3.8 ± 0.8 fold at week 9 and 12, respectively (Both $P < 0.01$) (**Figure 9B**). These reduced expression on gelatinases at the final stage and the greater changes in MMP-9 rather than MMP-2 corresponded with the results of gelatinases activity on zymogram.

3-8. Up-regulation of TIMPs activity

The proteolytic activity of MMPs can be regulated by TIMPs because of the inhibitive effect. Therefore, the relative abundances of TIMPs activity in the LV tissues were determined by reverse zymography (**Figure 10A**). TIMPs inhibitory activity resulted in dark blue bands compared with typical SDS-PAGE. In which TIMP-2, -3 and -4 were identified upon molecule weight as 21, 24 and 22 kDa respectively. However, predicted 29 kDa TIMP-1 was undetectable. Generally, the TIMPs activity increased along the process. A significant 4.5 ± 1.2 fold up-regulation of TIMP-2 was observed at week 12 (**Figure 10B**), the increase of TIMP-3 and TIMP-4 even earlier at week 5 ($P < 0.05$) (**Figure 10C and 10D**).

3-9. mRNA expression level of TIMPs

Comparing with the activity of TIMPs, the mRNAs of TIMPs in the LV tissues were also determined by semiquantitative RT-PCR (**Figure 11A**). In this analysis, the expression of GAPDH mRNA was used as internal control and the expression level were presented as fold

related to control at each time point. Except the 1.8 fold increase of TIMP-4 at week 9 and 12 ($P < 0.05$) (**Figure 11E**), there were no significant differences on mRNA expression of residual TIMPs in this study (**Figure 11B-D**).

.

IV. *Discussion*

Dox is a potent broad-spectrum anticancer drug and is crucial to the treatment of variety of solid and hematologic tumor such as acute leukemia, Hodgkin's and non-Hodgkin's lymphoma, and breast cancer (Takemura and Fujiwara, 2007). However, the well-known chronic cardiomyopathy of Dox greatly limits the usefulness. It may causes dilated cardiomyopathy in a dose-dependent manner and lead to heart failure in patients even after a long duration of discontinuous administration (Singal et al., 1997). Therefore, we attempted to utilize Dox to exam the hypothesis that alterations of ECM play a role in Dox-induced chronic cardiomyopathy and may be influenced by MMPs/TIMPs system. To our best knowledge, this issue has been studied rarely to this day.

In the present study we used a well-established murine model of Dox-induced cardiomyopathy. A low dosage administration by 4 mg/kg Dox hydrochloride per week was performed (**Figure 1**). Ultimately, five weeks treatment produced a 20 mg/kg accumulated dose and was equivalent to 1400 mg in a 70-kg man. In patients, the usual cumulative maximum dosage is about 500 mg/m^2, or 1000 mg for a 70-kg man. Beyond this dose, the frequency of cardiomyopathy rapidly escalates (Yi et al., 2006). Although the accumulated dose is highly related to the severity of cardiomyopathy, the greater dosage can lead to higher mortality due to several adverse effects such as diarrhea, weight loss, colitis, and bone marrow suppression (Van Vleet et al., 1979; Speth et al., 1988; Christiansen and Autschbach, 2006). In this study, the mortality came to about 30% during 12 weeks in Dox-treated mice. Most of them died in non-treated period, which reflected the long-term toxic effect of Dox.

Our results showed that Dox treatment in mice significantly reduced body weight (**Figure 2**), ventricle weight and the ventricle weight/tail length ratio (**Table 6**). Changes in body weight may result from the general toxicity of Dox (Klimtova et al., 2002), reduction of

food intake and inhibition of protein synthesis (Tong et al., 1991). The tail length of a rodent is a better indicator in malnutrition than body weight as a control (Kizaki et al., 2006). Therefore, we used ventricle weight/tail length ratio to estimate the Dox-induced cardiotoxicity. The decreases of ventricle weight and the ventricle weight/tail length ratio began from week 3 and further descended later, which may be the result of cardiomyocytes damage, Dox-induced apoptosis (Narula et al., 1996; Sharov et al., 1996) and inhibition of myocardial protein synthesis, confirming the prolonged cardiotoxic effects (Minotti et al., 2004).

Alteration of electrocardiogram on Dox-treated mice had been demonstrated previously (van Acker et al., 1996; Fisher et al., 2005). In our measurement, an increased S-T interval was observed in mice with Dox treatment and had a significant difference compared with control from week 5 initially (**Figure 3**). The prolongation of the repolarization phase may be related to the prolonged action potential in Purkinje fibers after incubation with Dox (le Marec et al., 1986). In another study, oxygen-derived free radicals generated by Dox can increase the duration of the action potential in isolated myocytes (Jabr and Cole, 1993). However, the increase of S-T interval in our study did not appear as early as the previous report (van Acker et al., 1996), which began after 2 weeks administration at a cumulative dose of 12 mg/kg. Additionally, the smaller degree of the increasing in this study at the relative time points, these may indicate a more moderate disorder in our mice. On the other hand, these divergences may also result from under anesthesia in different strain of mice.

In addition to ECG, we introduced a second cardiotoxic monitor by measuring the natriuretic peptides mRNA level in LV tissues (**Figure 4**). Synthesis and secretion of NPs by heart is responses to myocardial stretch due to volume expansion or pressure overload, and they are regarded as good biomarkers for the diagnosis of heart failure (Daniels and Maisel, 2007; Lainscak et al., 2007). The elevation of ANP and BNP in mRNA level in this study

provided evidence as hemodynamic deterioration which usually occur in heart failure (Daniels and Maisel, 2007). Nevertheless, the remarkable increase on ANP with a 1.5 fold slightly induced BNP may again indicate the moderate impairments on ventricular function rather than overt heart failure in our mice, and this difference may not be distinguished from NPs level in plasma (Langenickel et al., 2000).

By histology, the cytoplasmic vacuoles existed apparently in the cardiomyocytes of mice with Dox treatment after 12 weeks (**Figure 5**), it was consistent with that in patients (Takemura and Fujiwara, 2007). The morphology of the heart, however, showed no significant difference between the group of treatment and control. Typical dilation, representing the end stage remodeling of Dox-induced cardiomyopathy, was absent during the 12 weeks development in our study.

The mRNA expression level of type I and type III collagen in LV tissue was surveyed (**Figure 6**). The results showed no changes on these two predominant ECM components between Dox-treated and control groups. The consistent expression of collagen may result from the constitutional situations; however, we could not exclude the possibility that it was the antagonistic effect of profibrotic stimulations and Dox-induced oxidative stress which may decrease collagen synthesis and the abundance of mRNAs for procollagens (Tanaka et al., 1993; Siwik et al., 2001).

Consideration for ECM degradation, the expression and protein activity level of MMP-1, MMP-2, MMP-9 and TIMPs were measured. MMP-1 is one of the collagenase members which are the main enzymes as well as MT-MMP-1 capable of degrading intact fibrillar collagen (Ohuchi et al., 1997; Ala-aho and Kahari, 2005), suggesting MMP-1 is critical in tissue remodeling. However, it is interesting that this major collagenase in many species including human had been unable to identify in rodent until year 2001 (Balbin et al., 2001). Before the time, MMP-13 was the main interstitial collagenase in rodent, which had been

considered a counterpart to human MMP-1. Nowadays, the newly finding interstitial collagenases (Mcol-A and Mcol-B), the most possible orthologue of human MMP-1 finding so far, have been suggested playing roles in reproductive tissues in mice (Nuttall et al., 2004; Chen et al., 2007). However, few studies in cardiac related issues had been reported. The MMP-1 antibody used in this study recognizes an epitope from amino acid 332-350 of human MMP-1. Sequence of the recognizable site on human MMP-1 is highly similar to mice MMP-1 rather than MMP-13, and the specificity of the antibody for discrimination between mice MMP-1 and MMP-13 in myocardium had been mentioned in previous study (Seeland et al., 2007). In our finding by immunoblotting, the reduced 57 kDa latent MMP-1 accompanied by the increased 47 kDa active MMP-1 during the Dox treatment (**Figure 7**). This interesting opposite trends of changes began from the middle stage of the course and further altered later indicating the advanced activation of pro-MMP-1. However, the total MMP-1 protein was unchanged except at week 3. Recently, several studies reported the forming of ROS in the late onset cardiomyopathy even if the fact of intramyocardial short half-life of Dox and its metabolites (Lebrecht et al., 2003; Lebrecht et al., 2007). Other studies pointed that continuously induced ROS may be involved in MMPs activation by modification of the cysteine on MMPs propeptide domain (Fu et al., 2001; Okamoto et al., 2001; McCarthy et al., 2008). According to above, we supposed that the alteration of MMP-1 protein in our mice with Dox-induced cardiomyopathy was mainly due to posttranslational regulation and the activation may be partially associated with ROS induced by Dox. In addition, our finding may provide an explanation for the previous reports that the relative abundance of 57 kDa MMP-1 was significantly reduced (Thomas et al., 1998) but with increased collagenolytic activity (Gunja-Smith et al., 1996; Tyagi et al., 1996), at least partially contributed from active MMP-1, in patient with DCM. In this study, we found the activation of MMP-1 throughout the myocardium in Dox-induced cardiomyopathy, which may play an important role in ECM turnover and cardiac remodeling as well as human MMP-1 overexpression in mice (Kim et al.,

2000). Nevertheless, the transcript of MMP-1 based on the sequence from Balbin (Balbin et al., 2001) was limited to detection in heart of mice (Nuttall et al., 2004) and neither was our examination by PCR. Thus, the uncertainty of native MMP-1 in mice is necessary to be characterized further.

MMP-2 and MMP-9 so called gelatinases possess the capacity to degrade denatured collagen and a number of components from interstitial and basement membrane (Hijova, 2005). Moreover, intracardiomyocyte disorganization of the contractile apparatus in DCM by gelatinases was also reported (Rouet-Benzineb et al., 1999) suggesting the great importance of these MMPs in heart diseases. In this study, real-time PCR and zymography were used to determine the gelatinases expression level (**Figure 9**) and enzyme activity (**Figure 8**), respectively. At the end of the first week, the increased MMP-9 activity was observed with the unchanged MMP-2 mRNA and activity level. The results well connect with the previous studies, in which an early induced MMP-2 activity (Bai et al., 2004) and up-regulation of MMP-2 and MMP-9 mRNA expression in mice with acute Dox treatment were reported (Kizaki et al., 2006). According to the latter, the MMP-2 expression level returned to baseline earlier than MMP-9 at day 4 (Kizaki et al., 2006), it may interpret the later induced MMP-9 activity but not MMP-2 at day 6 in our case. This acute induction of gelatinases may be the respondence to inflammation induced by myocardium damage. In chronic phase, the activity of MMP-2 and MMP-9 was decreased at week 12 following the reduced mRNA expression at week 9. These unexpected results compared to most of the heart failure reports, usually up-regulation on gelatinases in heart failure, may be due to different stage of diseases and variant etiologies. For instance, MMP-2 was increased in nonischemic DCM but was unchanged in ischemic DCM (Spinale et al., 2000), and decreased MMP-9 mRNA expression with no differences in MMP-2 in DCM was also reported (Batlle et al., 2007). In addition to the reduction of both gelatinases, however, the smaller degree of alteration on MMP-2

displays stable and constitutive expression in myocardium (Spinale, 2007).

The activity of TIMPs was measured by reverse zymography (**Figure 10**). Three inhibitive bands were identified as TIMP-2,-3 and -4 according to molecular weight, which approximately increased at week 5 and further induced later. This increase of TIMPs at the protein activity was not coincident with the mRNA level (**Figure 11**) suggesting a role for posttranscriptional regulation.

V. *Conclusions*

In this study, we demonstrated a time-dependent alteration of MMPs/TIMPs in mouse LV with chronic Dox-induced cardiomyopathy. C57BL/6J mice were received 4 mg/kg Dox per week for five weeks, and the LV were harvested at week 1, 3, 5, 9 and 12 after first injection. The prolonged effect of Dox cardiotoxicity was revealed under the monitor by ECG and natriuretic peptides as well as the histological examination. Nevertheless, the hearts from Dox-treated mice showed no significant dilation suggesting that the end stage of the disease was absent during over 12 weeks administration. Besides the acute response of increased MMP-9 activity at first week, the reduction of mRNA expression and enzyme activity on MMP-2 and MMP-9 were present in the LV during end stage of this study. Both of gelatinases displayed similar alteration on zymogram; however, MMP-2 showed stable and constitutive expression relative to MMP-9. By detection of Western immunoblotting, a progressively opposite change of decreased latent MMP-1 with increased active MMP-1 over time was revealed. This up-regulated activation of MMP-1, might be a consequence of posttranslational modulation such as modification by Dox-induced ROS, is suggested to be a great contribution to ECM remodeling in HF. The inhibitory activity of TIMPs on reverse zymogram was up-regulated whereas with a generally constant pattern of gene expression suggesting a posttranscriptional regulation on TIMPs. In our findings, the identification of changes in certain species of MMPs and TIMPs may provide insight into the pathogenesis of cardiac remodeling in Dox-induced cardiomyopathy. However, there were several limitations in this study that must be recognized. First, according to the results of cardiotoxicity monitor and histology, the Dox-induced cardiomyopathy has not developed into end stage of HF. Therefore, the results revealed in this study provide information involved in evolution of Dox-induced cardiomyopathy rather than the end stage of the disease. Second, MMPs and TIMPs were assayed using semiquantitative immunoblotting or zymographic techniques.

Direct comparisons of changes in the levels of these proteins such as the ratio of MMPs/TIMPs in a stoichiometric fashion did not be performed. Third, the localization of the MMPs and TIMPs was not identified whereas the distribution pattern may be as important as the quantity in cardiac remodeling. Further studies are required to clarify the role of MMPs/TIMPs and established the mechanism involved in the Dox-induced cardiomyopathy.

VI. *References*

Ala-aho R, Kahari VM. 2005. Collagenases in cancer. Biochimie. 87:273-286.

Alves de Souza RC, Camacho AA. 2006. Neurohormonal, hemodynamic, and electrocardiographic evaluations of healthy dogs receiving long-term administration of doxorubicin. Am J Vet Res. 67:1319-1325.

Anand-Apte B, Bao L, Smith R, Iwata K, Olsen BR, Zetter B, Apte SS. 1996. A review of tissue inhibitor of metalloproteinases-3 (TIMP-3) and experimental analysis of its effect on primary tumor growth. Biochem Cell Biol. 74:853-862.

Bai P, Mabley JG, Liaudet L, Virag L, Szabo C, Pacher P. 2004. Matrix metalloproteinase activation is an early event in doxorubicin-induced cardiotoxicity. Oncol Rep. 11:505-508.

Baker AH, Edwards DR, Murphy G. 2002. Metalloproteinase inhibitors: biological actions and therapeutic opportunities. J Cell Sci. 115:3719-3727.

Balbin M, Fueyo A, Knauper V, Lopez JM, Alvarez J, Sanchez LM, Quesada V, Bordallo J, Murphy G, Lopez-Otin C. 2001. Identification and enzymatic characterization of two diverging murine counterparts of human interstitial collagenase (MMP-1) expressed at sites of embryo implantation. J Biol Chem. 276:10253-10262.

Batlle M, Perez-Villa F, Garcia-Pras E, Lazaro A, Orus J, Roque M, Roig E. 2007. Down-regulation of matrix metalloproteinase-9 (MMP-9) expression in the myocardium of congestive heart failure patients. Transplant Proc. 39:2344-2346.

Bauch M, Ester A, Kimura B, Victorica BE, Kedar A, Phillips MI. 1992. Atrial natriuretic peptide as a marker for doxorubicin-induced cardiotoxic effects. Cancer 69:1492-1497.

Bergman MR, Teerlink JR, Mahimkar R, Li L, Zhu BQ, Nguyen A, Dahi S, Karliner JS, Lovett DH. 2007. Cardiac matrix metalloproteinase-2 expression independently induces marked ventricular remodeling and systolic dysfunction. Am J Physiol Heart Circ Physiol. 292:H1847-1860.

Borer JS, Truter S, Herrold EM, Falcone DJ, Pena M, Carter JN, Dumlao TF, Lee JA, Supino PG. 2002. Myocardial fibrosis in chronic aortic regurgitation: molecular and cellular responses to volume overload. Circulation 105:1837-1842.

Boucek RJ, Jr., Miracle A, Anderson M, Engelman R, Atkinson J, Dodd DA. 1999. Persistent effects of doxorubicin on cardiac gene expression. J Mol Cell Cardiol. 31:1435-1446.

Brew K, Dinakarpandian D, Nagase H. 2000. Tissue inhibitors of metalloproteinases:

evolution, structure and function. Biochim Biophys Acta 1477:267-283.

Brilla CG, Rupp H. 1994. Myocardial collagen matrix remodeling and congestive heart failure. Cardiologia. 39:389-393.

Bryant J, Picot J, Baxter L, Levitt G, Sullivan I, Clegg A. 2007. Use of cardiac markers to assess the toxic effects of anthracyclines given to children with cancer: a systematic review. Eur J Cancer. 43:1959-1966.

Carmeli E, Moas M, Reznick AZ, Coleman R. 2004. Matrix metalloproteinases and skeletal muscle: a brief review. Muscle Nerve. 29:191-197.

Chen L, Nakai M, Belton RJ, Jr., Nowak RA. 2007. Expression of extracellular matrix metalloproteinase inducer and matrix metalloproteinases during mouse embryonic development. Reproduction 133:405-414.

Chen MM, Lam A, Abraham JA, Schreiner GF, Joly AH. 2000. CTGF expression is induced by TGF- beta in cardiac fibroblasts and cardiac myocytes: a potential role in heart fibrosis. J Mol Cell Cardiol. 32:1805-1819.

Christiansen S, Autschbach R. 2006. Doxorubicin in experimental and clinical heart failure. Eur J Cardiothorac Surg. 30:611-616.

Cohn JN, Ferrari R, Sharpe N. 2000. Cardiac remodeling--concepts and clinical implications: a consensus paper from an international forum on cardiac remodeling. Behalf of an International Forum on Cardiac Remodeling. J Am Coll Cardiol. 35:569-582.

Coker ML, Doscher MA, Thomas CV, Galis ZS, Spinale FG. 1999. Matrix metalloproteinase synthesis and expression in isolated LV myocyte preparations. Am J Physiol. 277:H777-787.

Cook TF, Burke JS, Bergman KD, Quinn CO, Jeffrey JJ, Partridge NC. 1994. Cloning and regulation of rat tissue inhibitor of metalloproteinases-2 in osteoblastic cells. Arch Biochem Biophys. 311:313-320.

Creemers EE, Davis JN, Parkhurst AM, Leenders P, Dowdy KB, Hapke E, Hauet AM, Escobar PG, Cleutjens JP, Smits JF, Daemen MJ, Zile MR, Spinale FG. 2003. Deficiency of TIMP-1 exacerbates LV remodeling after myocardial infarction in mice. Am J Physiol Heart Circ Physiol. 284:H364-371.

Cucoranu I, Clempus R, Dikalova A, Phelan PJ, Ariyan S, Dikalov S, Sorescu D. 2005. NAD(P)H oxidase 4 mediates transforming growth factor-beta1-induced differentiation of cardiac fibroblasts into myofibroblasts. Circ Res. 97:900-907.

Daniels LB, Maisel AS. 2007. Natriuretic peptides. J Am Coll Cardiol. 50:2357-2368.

de Bold AJ, Borenstein HB, Veress AT, Sonnenberg H. 1981. A rapid and potent natriuretic response to intravenous injection of atrial myocardial extract in rats. Life Sci. 28:89-94.

de Bold AJ. 1985. Atrial natriuretic factor: a hormone produced by the heart. Science 230:767-770.

de Souza RCA, Camacho AA. 2006. Neurohormonal, hemodynamic, and electrocardiographic evaluations of healthy dogs receiving long-term administration of doxorubicin (vol 67, pg 1319, 2006). Am J Vet Res. 67:1779-1779.

Delgado RM, 3rd, Nawar MA, Zewail AM, Kar B, Vaughn WK, Wu KK, Aleksic N, Sivasubramanian N, McKay K, Mann DL, Willerson JT. 2004. Cyclooxygenase-2 inhibitor treatment improves left ventricular function and mortality in a murine model of doxorubicin-induced heart failure. Circulation 109:1428-433.

Dollery CM, McEwan JR, Henney AM. 1995. Matrix metalloproteinases and cardiovascular disease. Circ Res. 77:863-868.

Doroshow JH. 1983. Effect of anthracycline antibiotics on oxygen radical formation in rat heart. Cancer Res. 43:460-472.

Ducharme A, Frantz S, Aikawa M, Rabkin E, Lindsey M, Rohde LE, Schoen FJ, Kelly RA, Werb Z, Libby P, Lee RT. 2000. Targeted deletion of matrix metalloproteinase-9 attenuates left ventricular enlargement and collagen accumulation after experimental myocardial infarction. J Clin Invest. 106:55-62.

Fedak PW, Smookler DS, Kassiri Z, Ohno N, Leco KJ, Verma S, Mickle DA, Watson KL, Hojilla CV, Cruz W, Weisel RD, Li RK, Khokha R. 2004. TIMP-3 deficiency leads to dilated cardiomyopathy. Circulation 110:2401-2409.

Fedarko NS, Jain A, Karadag A, Fisher LW. 2004. Three small integrin binding ligand N-linked glycoproteins (SIBLINGs) bind and activate specific matrix metalloproteinases. FASEB J. 18:734-736.

Feldman AM, Li YY, McTiernan CF. 2001. Matrix metalloproteinases in pathophysiology and treatment of heart failure. Lancet 357:654-655.

Fernandez CA, Yan L, Louis G, Yang J, Kutok JL, Moses MA. 2005. The matrix metalloproteinase-9/neutrophil gelatinase-associated lipocalin complex plays a role in breast tumor growth and is present in the urine of breast cancer patients. Clin Cancer Res. 11:5390-5395.

Fisher PW, Salloum F, Das A, Hyder H, Kukreja RC. 2005. Phosphodiesterase-5 inhibition with sildenafil attenuates cardiomyocyte apoptosis and left ventricular dysfunction in a

chronic model of doxorubicin cardiotoxicity. Circulation 111:1601-1610.

Fu X, Kassim SY, Parks WC, Heinecke JW. 2001. Hypochlorous acid oxygenates the cysteine switch domain of pro-matrilysin (MMP-7). A mechanism for matrix metalloproteinase activation and atherosclerotic plaque rupture by myeloperoxidase. J Biol Chem. 276:41279-41287.

Gewirtz DA. 1999. A critical evaluation of the mechanisms of action proposed for the antitumor effects of the anthracycline antibiotics adriamycin and daunorubicin. Biochem Pharmacol. 57:727-741.

Goldberg GI, Wilhelm SM, Kronberger A, Bauer EA, Grant GA, Eisen AZ. 1986. Human fibroblast collagenase. Complete primary structure and homology to an oncogene transformation-induced rat protein. J Biol Chem. 261:6600-6605.

Greene J, Wang M, Liu YE, Raymond LA, Rosen C, Shi YE. 1996. Molecular cloning and characterization of human tissue inhibitor of metalloproteinase 4. J Biol Chem. 271:30375-30380.

Gross J, Lapiere CM. 1962. Collagenolytic activity in amphibian tissues: a tissue culture assay. Proc Natl Acad Sci USA. 48:1014-1022.

Gunja-Smith Z, Morales AR, Romanelli R, Woessner JF, Jr. 1996. Remodeling of human myocardial collagen in idiopathic dilated cardiomyopathy. Role of metalloproteinases and pyridinoline cross-links. Am J Pathol. 148:1639-1648.

Hayakawa H, Komada Y, Hirayama M, Hori H, Ito M, Sakurai M. 2001. Plasma levels of natriuretic peptides in relation to doxorubicin-induced cardiotoxicity and cardiac function in children with cancer. Med Pediatr Oncol. 37:4-9.

Hayashidani S, Tsutsui H, Ikeuchi M, Shiomi T, Matsusaka H, Kubota T, Imanaka-Yoshida K, Itoh T, Takeshita A. 2003. Targeted deletion of MMP-2 attenuates early LV rupture and late remodeling after experimental myocardial infarction. Am J Physiol Heart Circ Physiol. 285:H1229-1235.

Heymans S, Luttun A, Nuyens D, Theilmeier G, Creemers E, Moons L, Dyspersin GD, Cleutjens JP, Shipley M, Angellilo A, Levi M, Nube O, Baker A, Keshet E, Lupu F, Herbert JM, Smits JF, Shapiro SD, Baes M, Borgers M, Collen D, Daemen MJ, Carmeliet P. 1999. Inhibition of plasminogen activators or matrix metalloproteinases prevents cardiac rupture but impairs therapeutic angiogenesis and causes cardiac failure. Nat Med. 5:1135-1142.

Hijova E. 2005. Matrix metalloproteinases: their biological functions and clinical implications. Bratisl Lek Listy. 106:127-132.

Horwitz AL, Hance AJ, Crystal RG. 1977. Granulocyte collagenase: selective digestion of type I relative to type III collagen. Proc Natl Acad Sci USA. 74:897-901.

Huang ZQ, Li HX, Wang JL, Wan SG. 2004. [Clinical observation of electrocardiographic changes in response to taxotere combined with adriamycin treatment for breast cancer]. Di Yi Jun Yi Da Xue Xue Bao. 24:582-583.

Hunt SA. 2005. ACC/AHA 2005 guideline update for the diagnosis and management of chronic heart failure in the adult: a report of the American College of Cardiology/American Heart Association Task Force on Practice Guidelines (Writing Committee to Update the 2001 Guidelines for the Evaluation and Management of Heart Failure). J Am Coll Cardiol. 46:e1-82.

Ikonomidis JS, Hendrick JW, Parkhurst AM, Herron AR, Escobar PG, Dowdy KB, Stroud RE, Hapke E, Zile MR, Spinale FG. 2005. Accelerated LV remodeling after myocardial infarction in TIMP-1-deficient mice: effects of exogenous MMP inhibition. Am J Physiol Heart Circ Physiol. 288:H149-158.

Ito H, Rucker E, Steplewski A, McAdams E, Brittingham RJ, Alabyeva T, Fertala A. 2005. Guilty by association: some collagen II mutants alter the formation of ECM as a result of atypical interaction with fibronectin. J Mol Biol. 352:382-395.

Jabr RI, Cole WC. 1993. Alterations in electrical activity and membrane currents induced by intracellular oxygen-derived free radical stress in guinea pig ventricular myocytes. Circ Res. 72:1229-1244.

Janicki JS, Brower GL. 2002. The role of myocardial fibrillar collagen in ventricular remodeling and function. J Card Fail. 8:S319-325.

Jayasankar V, Woo YJ, Bish LT, Pirolli TJ, Berry MF, Burdick J, Bhalla RC, Sharma RV, Gardner TJ, Sweeney HL. 2004. Inhibition of matrix metalloproteinase activity by TIMP-1 gene transfer effectively treats ischemic cardiomyopathy. Circulation 110:II180-186.

Jones CB, Sane DC, Herrington DM. 2003. Matrix metalloproteinases: a review of their structure and role in acute coronary syndrome. Cardiovasc Res. 59:812-823.

Kai H, Kuwahara F, Tokuda K, Imaizumi T. 2005. Diastolic dysfunction in hypertensive hearts: roles of perivascular inflammation and reactive myocardial fibrosis. Hypertens Res. 28:483-490.

Kalyanaraman B, Perez-Reyes E, Mason RP. 1980. Spin-trapping and direct electron spin resonance investigations of the redox metabolism of quinone anticancer drugs. Biochim Biophys Acta 630:119-130.

Kassiri Z, Khokha R. 2005. Myocardial extra-cellular matrix and its regulation by metalloproteinases and their inhibitors. Thromb Haemost. 93:212-219.

Kim HE, Dalal SS, Young E, Legato MJ, Weisfeldt ML, D'Armiento J. 2000. Disruption of the myocardial extracellular matrix leads to cardiac dysfunction. J Clin Invest. 106:857-866.

Kizaki K, Ito R, Okada M, Yoshioka K, Uchide T, Temma K, Mutoh K, Uechi M, Hara Y. 2006. Enhanced gene expression of myocardial matrix metalloproteinases 2 and 9 after acute treatment with doxorubicin in mice. Pharmacol Res. 53:341-346.

Klimtova I, Simunek T, Mazurova Y, Hrdina R, Gersl V, Adamcova M. 2002. Comparative study of chronic toxic effects of daunorubicin and doxorubicin in rabbits. Hum Exp Toxicol. 21:649-657.

Koh E, Nakamura T, Takahashi H. 2004. Troponin-T and brain natriuretic peptide as predictors for adriamycin-induced cardiomyopathy in rats. Circ J. 68:163-167.

Kostin S, Hein S, Arnon E, Scholz D, Schaper J. 2000. The cytoskeleton and related proteins in the human failing heart. Heart Fail Rev. 5:271-280.

Lainscak M, von Haehling S, Springer J, Anker SD. 2007. Biomarkers for chronic heart failure. Heart Fail Monit. 5:77-82.

Langenickel T, Pagel I, Hohnel K, Dietz R, Willenbrock R. 2000. Differential regulation of cardiac ANP and BNP mRNA in different stages of experimental heart failure. Am J Physiol Heart Circ Physiol. 278:H1500-1506.

le Marec H, Spinelli W, Rosen MR. 1986. The effects of doxorubicin on ventricular tachycardia. Circulation 74:881-889.

Lebrecht D, Setzer B, Ketelsen UP, Haberstroh J, Walker UA. 2003. Time-dependent and tissue-specific accumulation of mtDNA and respiratory chain defects in chronic doxorubicin cardiomyopathy. Circulation 108:2423-2429.

Lebrecht D, Geist A, Ketelsen UP, Haberstroh J, Setzer B, Walker UA. 2007. Dexrazoxane prevents doxorubicin-induced long-term cardiotoxicity and protects myocardial mitochondria from genetic and functional lesions in rats. Br J Pharmacol. 151:771-778.

Lee AY, Akers KT, Collier M, Li L, Eisen AZ, Seltzer JL. 1997. Intracellular activation of gelatinase A (72-kDa type IV collagenase) by normal fibroblasts. Proc Natl Acad Sci USA. 94:4424-4429.

Leri A, Kajstura J, Anversa P. 2005. Cardiac stem cells and mechanisms of myocardial regeneration. Physiol Rev. 85:1373-1416.

Li YY, Feldman AM, Sun Y, McTiernan CF. 1998. Differential expression of tissue inhibitors of metalloproteinases in the failing human heart. Circulation 98:1728-1734.

Li YY, McTiernan CF, Feldman AM. 1999. Proinflammatory cytokines regulate tissue inhibitors of metalloproteinases and disintegrin metalloproteinase in cardiac cells. Cardiovasc Res. 42:162-172.

Li YY, McTiernan CF, Feldman AM. 2000. Interplay of matrix metalloproteinases, tissue inhibitors of metalloproteinases and their regulators in cardiac matrix remodeling. Cardiovasc Res. 46:214-224.

Libson AM, Gittis AG, Collier IE, Marmer BL, Goldberg GI, Lattman EE. 1995. Crystal structure of the haemopexin-like C-terminal domain of gelatinase A. Nat Struct Biol. 2:938-942.

Livak KJ, Schmittgen TD. 2001. Analysis of relative gene expression data using real-time quantitative PCR and the 2(-Delta Delta C(T)) Method. Methods 25:402-408.

Lombard C, Saulnier J, Wallach J. 2005. Assays of matrix metalloproteinases (MMPs) activities: a review. Biochimie. 87:265-272.

MacKenna D, Summerour SR, Villarreal FJ. 2000. Role of mechanical factors in modulating cardiac fibroblast function and extracellular matrix synthesis. Cardiovasc Res. 46:257-263.

Makowski GS, Ramsby ML. 1998. Identification and partial characterization of three calcium- and zinc-independent gelatinases constitutively present in human circulation. Biochem Mol Biol Int. 46:1043-1053.

Manabe I, Shindo T, Nagai R. 2002. Gene expression in fibroblasts and fibrosis: involvement in cardiac hypertrophy. Circ Res. 91:1103-1113.

Maquart FX, Pickart L, Laurent M, Gillery P, Monboisse JC, Borel JP. 1988. Stimulation of collagen synthesis in fibroblast cultures by the tripeptide-copper complex glycyl-L-histidyl-L-lysine-Cu2+. FEBS Lett. 238:343-346.

Mathew ST, Gottdiener JS, Kitzman D, Aurigemma G. 2004. Congestive heart failure in the elderly: the Cardiovascular Health Study. Am J Geriatr Cardiol. 13:61-68.

Matsumura S, Iwanaga S, Mochizuki S, Okamoto H, Ogawa S, Okada Y. 2005. Targeted deletion or pharmacological inhibition of MMP-2 prevents cardiac rupture after myocardial infarction in mice. J Clin Invest. 115:599-609.

Matsusaka H, Ide T, Matsushima S, Ikeuchi M, Kubota T, Sunagawa K, Kinugawa S, Tsutsui H. 2006. Targeted deletion of matrix metalloproteinase 2 ameliorates myocardial

remodeling in mice with chronic pressure overload. Hypertension 47:711-717.

McCarthy SM, Bove PF, Matthews DE, Akaike T, van der Vliet A. 2008. Nitric oxide regulation of MMP-9 activation and its relationship to modifications of the cysteine switch. Biochemistry 47:5832-5840.

Minotti G, Menna P, Salvatorelli E, Cairo G, Gianni L. 2004. Anthracyclines: molecular advances and pharmacologic developments in antitumor activity and cardiotoxicity. Pharmacol Rev. 56:185-229.

Morgunova E, Tuuttila A, Bergmann U, Isupov M, Lindqvist Y, Schneider G, Tryggvason K. 1999. Structure of human pro-matrix metalloproteinase-2: activation mechanism revealed. Science 284:1667-1670.

Moshal KS, Tyagi N, Moss V, Henderson B, Steed M, Ovechkin A, Aru GM, Tyagi SC. 2005. Early induction of matrix metalloproteinase-9 transduces signaling in human heart end stage failure. J Cell Mol Med. 9:704-713.

Mukoyama M, Nakao K, Hosoda K, Suga S, Saito Y, Ogawa Y, Shirakami G, Jougasaki M, Obata K, Yasue H. 1991. Brain natriuretic peptide as a novel cardiac hormone in humans. Evidence for an exquisite dual natriuretic peptide system, atrial natriuretic peptide and brain natriuretic peptide. J Clin Invest. 87:1402-1412.

Murphy G, Bretz U, Baggiolini M, Reynolds JJ. 1980. The latent collagenase and gelatinase of human polymorphonuclear neutrophil leucocytes. Biochem J. 192:517-525.

Nagase H, Woessner JF, Jr. 1999. Matrix metalloproteinases. J Biol Chem. 274:21491-21494.

Nakao K, Ogawa Y, Suga S, Imura H. 1992. Molecular biology and biochemistry of the natriuretic peptide system. II: Natriuretic peptide receptors. J Hypertens. 10:1111-1114.

Narula J, Haider N, Virmani R, DiSalvo TG, Kolodgie FD, Hajjar RJ, Schmidt U, Semigran MJ, Dec GW, Khaw BA. 1996. Apoptosis in myocytes in end-stage heart failure. N Engl J Med. 335:1182-1189.

Nousiainen T, Vanninen E, Rantala A, Jantunen E, Hartikainen J. 1999. QT dispersion and late potentials during doxorubicin therapy for non-Hodgkin's lymphoma. J Intern Med. 245:359-364.

Nuttall RK, Sampieri CL, Pennington CJ, Gill SE, Schultz GA, Edwards DR. 2004. Expression analysis of the entire MMP and TIMP gene families during mouse tissue development. FEBS Lett. 563:129-134.

Odom AL, Hatwig CA, Stanley JS, Benson AM. 1992. Biochemical determinants of Adriamycin toxicity in mouse liver, heart and intestine. Biochem Pharmacol.

43:831-836.

Ohuchi E, Imai K, Fujii Y, Sato H, Seiki M, Okada Y. 1997. Membrane type 1 matrix metalloproteinase digests interstitial collagens and other extracellular matrix macromolecules. J Biol Chem. 272:2446-2451.

Okada A, Garnier JM, Vicaire S, Basset P. 1994. Cloning of the cDNA encoding rat tissue inhibitor of metalloproteinase 1 (TIMP-1), amino acid comparison with other TIMPs, and gene expression in rat tissues. Gene. 147:301-302.

Okamoto T, Akaike T, Sawa T, Miyamoto Y, van der Vliet A, Maeda H. 2001. Activation of matrix metalloproteinases by peroxynitrite-induced protein S-glutathiolation via disulfide S-oxide formation. J Biol Chem. 276:29596-29602.

Oliver GW, Leferson JD, Stetler-Stevenson WG, Kleiner DE. 1997. Quantitative reverse zymography: analysis of picogram amounts of metalloproteinase inhibitors using gelatinase A and B reverse zymograms. Anal Biochem. 244:161-166.

Overall CM, King AE, Sam DK, Ong AD, Lau TT, Wallon UM, DeClerck YA, Atherstone J. 1999. Identification of the tissue inhibitor of metalloproteinases-2 (TIMP-2) binding site on the hemopexin carboxyl domain of human gelatinase A by site-directed mutagenesis. The hierarchical role in binding TIMP-2 of the unique cationic clusters of hemopexin modules III and IV. J Biol Chem. 274:4421-4429.

Pinarli FG, Oguz A, Tunaoglu FS, Karadeniz C, Gokcora N, Elbeg S. 2005. Late cardiac evaluation of children with solid tumors after anthracycline chemotherapy. Pediatr Blood Cancer 44:370-377.

Puri A, Maulik SK, Ray R, Bhatnagar V. 2005. Electrocardiographic and biochemical evidence for the cardioprotective effect of vitamin E in doxorubicin-induced acute cardiotoxicity in rats. Eur J Pediatr Surg. 15:387-391.

Rahman A, Alam M, Rao S, Cai L, Clark LT, Shafiq S, Siddiqui MA. 2001. Differential effects of doxorubicin on atrial natriuretic peptide expression in vivo and in vitro. Biol Res. 34:195-206.

Roeb E, Matern S. 2001. Matrix metalloproteinases: Promoters of tumor invasion and metastasis - A review with focus on gastrointestinal tumors. Z Gastroenterol. 39:807-813.

Romanic AM, Harrison SM, Bao W, Burns-Kurtis CL, Pickering S, Gu J, Grau E, Mao J, Sathe GM, Ohlstein EH, Yue TL. 2002. Myocardial protection from ischemia/reperfusion injury by targeted deletion of matrix metalloproteinase-9. Cardiovasc Res. 54:549-558.

Roten L, Nemoto S, Simsic J, Coker ML, Rao V, Baicu S, Defreyte G, Soloway PJ, Zile MR,

Spinale FG. 2000. Effects of gene deletion of the tissue inhibitor of the matrix metalloproteinase-type 1 (TIMP-1) on left ventricular geometry and function in mice. J Mol Cell Cardiol. 32:109-120.

Rouet-Benzineb P, Buhler JM, Dreyfus P, Delcourt A, Dorent R, Perennec J, Crozatier B, Harf A, Lafuma C. 1999. Altered balance between matrix gelatinases (MMP-2 and MMP-9) and their tissue inhibitors in human dilated cardiomyopathy: potential role of MMP-9 in myosin-heavy chain degradation. Eur J Heart Fail. 1:337-352.

Sabbah HN, Sharov VG, Lesch M, Goldstein S. 1995. Progression of heart failure: a role for interstitial fibrosis. Mol Cell Biochem. 147:29-34.

Sacco G, Bigioni M, Evangelista S, Goso C, Manzini S, Maggi CA. 2001. Cardioprotective effects of zofenopril, a new angiotensin-converting enzyme inhibitor, on doxorubicin-induced cardiotoxicity in the rat. Eur J Pharmacol. 414:71-78.

Sakyo K, Kobayashi J, Ito A, Mori Y. 1983. Partial purification and characterization of gelatinase and metal dependent peptidase from rabbit uterus and their synergistic action on gelatin in vitro. J Biochem. 94:1913-1923.

Schnee JM, Hsueh WA. 2000. Angiotensin II, adhesion, and cardiac fibrosis. Cardiovasc Res. 46:264-268.

Schulz R. 2007. Intracellular targets of matrix metalloproteinase-2 in cardiac disease: rationale and therapeutic approaches. Annu Rev Pharmacol Toxicol. 47:211-242.

Seeland U, Selejan S, Engelhardt S, Muller P, Lohse MJ, Bohm M. 2007. Interstitial remodeling in beta1-adrenergic receptor transgenic mice. Basic Res Cardiol. 102:183-193.

Sellers A, Reynolds JJ, Meikle MC. 1978. Neutral metallo-proteinases of rabbit bone. Separation in latent forms of distinct enzymes that when activated degrade collagen, gelatin and proteoglycans. Biochem J. 171:493-496.

Sharov VG, Sabbah HN, Shimoyama H, Goussev AV, Lesch M, Goldstein S. 1996. Evidence of cardiocyte apoptosis in myocardium of dogs with chronic heart failure. Am J Pathol. 148:141-149.

Silbiger SM, Jacobsen VL, Cupples RL, Koski RA. 1994. Cloning of cDNAs encoding human TIMP-3, a novel member of the tissue inhibitor of metalloproteinase family. Gene 141:293-297.

Singal PK, Segstro RJ, Singh RP, Kutryk MJ. 1985. Changes in lysosomal morphology and enzyme activities during the development of adriamycin-induced cardiomyopathy. Can J

Cardiol. 1:139-147.

Singal PK, Deally CM, Weinberg LE. 1987. Subcellular effects of adriamycin in the heart: a concise review. J Mol Cell Cardiol. 19:817-828.

Singal PK, Iliskovic N, Li T, Kumar D. 1997. Adriamycin cardiomyopathy: pathophysiology and prevention. FASEB J. 11:931-936.

Singal PK, Iliskovic N. 1998. Doxorubicin-induced cardiomyopathy. N Engl J Med. 339:900-905.

Sivakumar P, Gupta S, Sarkar S, Sen S. 2008. Upregulation of lysyl oxidase and MMPs during cardiac remodeling in human dilated cardiomyopathy. Mol Cell Biochem. 307:159-167.

Siwik DA, Pagano PJ, Colucci WS. 2001. Oxidative stress regulates collagen synthesis and matrix metalloproteinase activity in cardiac fibroblasts. Am J Physiol Cell Physiol. 280:C53-60.

Soker M, Kervancioglu M. 2005. Plasma concentrations of NT-pro-BNP and cardiac troponin-I in relation to doxorubicin-induced cardiomyopathy and cardiac function in childhood malignancy. Saudi Med J. 26:1197-1202.

Sopata I, Wize J. 1979. A latent gelatin specific proteinase of human leucocytes and its activation. Biochim Biophys Acta 571:305-312.

Speth PA, van Hoesel QG, Haanen C. 1988. Clinical pharmacokinetics of doxorubicin. Clin Pharmacokinet. 15:15-31.

Spinale FG, Coker ML, Heung LJ, Bond BR, Gunasinghe HR, Etoh T, Goldberg AT, Zellner JL, Crumbley AJ. 2000. A matrix metalloproteinase induction/activation system exists in the human left ventricular myocardium and is upregulated in heart failure. Circulation 102:1944-1949.

Spinale FG. 2007. Myocardial matrix remodeling and the matrix metalloproteinases: influence on cardiac form and function. Physiol Rev. 87:1285-1342.

Stawowy P, Margeta C, Kallisch H, Seidah NG, Chretien M, Fleck E, Graf K. 2004. Regulation of matrix metalloproteinase MT1-MMP/MMP-2 in cardiac fibroblasts by TGF-beta1 involves furin-convertase. Cardiovasc Res. 63:87-97.

Stefanidakis M, Koivunen E. 2006. Cell-surface association between matrix metalloproteinases and integrins: role of the complexes in leukocyte migration and cancer progression. Blood 108:1441-1450.

Stetler-Stevenson WG, Krutzsch HC, Liotta LA. 1989. Tissue inhibitor of metalloproteinase (TIMP-2). A new member of the metalloproteinase inhibitor family. J Biol Chem. 264:17374-17378.

Sun Y, Weber KT. 2005. Animal models of cardiac fibrosis. Methods Mol Med. 117:273-90.

Swynghedauw B. 1999. Molecular mechanisms of myocardial remodeling. Physiol Rev. 79:215-262.

Taipale J, Keski-Oja J. 1997. Growth factors in the extracellular matrix. FASEB J. 11:51-59.

Takemura G, Fujiwara H. 2007. Doxorubicin-induced cardiomyopathy from the cardiotoxic mechanisms to management. Prog Cardiovasc Dis. 49:330-352.

Tanaka H, Okada T, Konishi H, Tsuji T. 1993. The effect of reactive oxygen species on the biosynthesis of collagen and glycosaminoglycans in cultured human dermal fibroblasts. Arch Dermatol Res. 285:352-355.

Thomas CV, Coker ML, Zellner JL, Handy JR, Crumbley AJ, 3rd, Spinale FG. 1998. Increased matrix metalloproteinase activity and selective upregulation in LV myocardium from patients with end-stage dilated cardiomyopathy. Circulation 97:1708-1715.

Tikanoja T, Riikonen P, Perkkio M, Helenius T. 1998. Serum N-terminal atrial natriuretic peptide (NT-ANP) in the cardiac follow-up in children with cancer. Med Pediatr Oncol. 31:73-78.

Tong J, Ganguly PK, Singal PK. 1991. Myocardial adrenergic changes at two stages of heart failure due to adriamycin treatment in rats. Am J Physiol. 260:H909-916.

Torrado M, Lopez E, Centeno A, Medrano C, Castro-Beiras A, Mikhailov AT. 2003. Myocardin mRNA is augmented in the failing myocardium: expression profiling in the porcine model and human dilated cardiomyopathy. J Mol Med. 81:566-577.

Tyagi SC, Campbell SE, Reddy HK, Tjahja E, Voelker DJ. 1996. Matrix metalloproteinase activity expression in infarcted, noninfarcted and dilated cardiomyopathic human hearts. Mol Cell Biochem. 155:13-21.

van Acker SA, Kramer K, Voest EE, Grimbergen JA, Zhang J, van der Vijgh WJ, Bast A. 1996. Doxorubicin-induced cardiotoxicity monitored by ECG in freely moving mice. A new model to test potential protectors. Cancer Chemother Pharmacol. 38:95-101.

Van Vleet JF, Greenwood LA, Ferrans VJ. 1979. Pathologic features of adriamycin toxicosis in young pigs: nonskeletal lesions. Am J Vet Res. 40:1537-1552.

Van Vleet JF, Ferrans VJ. 1980. Clinical and pathologic features of chronic adriamycin toxicosis in rabbits. Am J Vet Res. 41:1462-1469.

van Wart HE, Birkedal-Hansen H. 1990. The cysteine switch: a principle of regulation of metalloproteinase activity with potential applicability to the entire matrix metalloproteinase gene family. Proc Natl Acad Sci USA. 87:5578-5582.

Wallon UM, Overall CM. 1997. The hemopexin-like domain (C domain) of human gelatinase A (matrix metalloproteinase-2) requires Ca2+ for fibronectin and heparin binding. Binding properties of recombinant gelatinase A C domain to extracellular matrix and basement membrane components. J Biol Chem. 272:7473-7481.

Wei CM, Heublein DM, Perrella MA, Lerman A, Rodeheffer RJ, McGregor CG, Edwards WD, Schaff HV, Burnett JC, Jr. 1993. Natriuretic peptide system in human heart failure. Circulation 88:1004-1009.

Weiss RB. 1992. The anthracyclines: will we ever find a better doxorubicin? Semin Oncol. 19:670-686.

Whittaker P. 1995. Unravelling the mysteries of collagen and cicatrix after myocardial infarction. Cardiovasc Res. 29:758-762.

Wilhelm SM, Eisen AZ, Teter M, Clark SD, Kronberger A, Goldberg G. 1986. Human fibroblast collagenase: glycosylation and tissue-specific levels of enzyme synthesis. Proc Natl Acad Sci USA. 83:3756-3760.

Yasue H, Yoshimura M, Sumida H, Kikuta K, Kugiyama K, Jougasaki M, Ogawa H, Okumura K, Mukoyama M, Nakao K. 1994. Localization and mechanism of secretion of B-type natriuretic peptide in comparison with those of A-type natriuretic peptide in normal subjects and patients with heart failure. Circulation 90:195-203.

Yi X, Bekeredjian R, DeFilippis NJ, Siddiquee Z, Fernandez E, Shohet RV. 2006. Transcriptional analysis of doxorubicin-induced cardiotoxicity. Am J Physiol Heart Circ Physiol. 290:H1098-1102.

Zannad F, Radauceanu A. 2005. Effect of MR blockade on collagen formation and cardiovascular disease with a specific emphasis on heart failure. Heart Fail Rev. 10:71-78.

Table 1. Regulations of MMPs and TIMPs in the hearts with dilated cardiomyopathy (DCM)

Disease	Key findings	Reference
Idiopathic DCM	Neutrophil-type collagenase activity elevated 30X as is the activity of gelatinase; Tissue inhibitor of metalloproteinase activity falls to negligible; Doubling of collagen concentration; Diminished mature cross-link	Gunja-Smith et al., 1996
Idiopathic DCM	Zymographic activity, MMP-3 and 92 kDa MMP-9 increased; 57 kDa MMP-1 decreased; 72 kDa MMP-2 was unchanged; TIMP-1 and TIMP-2 increased	Thomas et al., 1998
Ischemic/Idiopathic DCM	MMP-9 protein content and total gelatinolytic activity were upregulated; TIMP-1 and -3 transcripts and proteins was reduced in ICM and DCM; TIMP-4 protein was reduced in ICM	Li et al., 1998
DCM	Gel zymography revealed similar activity of MMP-2 and MMP-9; All TIMPs were down-regulated	Rouet-Benzineb et al., 1999
Ischemic/Idiopathic DCM	Zymography MMP activity, EMMPRIN, MT1-MMP and MMP-9 increased with both nonischemic DCM and ischemic DCM; MMP-2 and MMP-3 increased with nonischemic DCM; MMP-1 levels decreased with both forms of DCM	Spinale et al., 2000
DCM	MMP-2 and MMP-9 were increased significantly; TIMP 1, and 2 were significantly up-regulated (mRNA); Increase in Type I (18%) and Type III (33%) collagen	Sivakumar et al., 2008

ICM, ischemic cardiomyopathy; DCM, dilated cardiomyopathy**;** EMMPRIN, extracellular matrix metalloproteinase inducer

Table 2. Physiological functions of MMPs and TIMPs in transgenic animals

Experimental model	Key findings	Reference
MMP-2 knockout in mice with MI	Reduced LV dilation; improved fractional shortening; lower incidence of LV rupture after MI	Hayashidani et al., 2003
MMP-2 knockout in mice with MI	Reduction in macrophage infiltration; Preventing cardiac rupture and delays post-MI remodeling	Matsumura et al., 2005
MMP-2 knockout in mice with chronic pressure overload	Attenuation of interstitial fibrosis, LV hypertrophy and dysfunction	Matsusaka et al., 2006
MMP-9 knockout in mice with MI	Less collagen accumulation in the infarcted area; Enhanced expression of MMP-2, MMP-13, and TIMP-1 and a reduced number of macrophages; Attenuation of LV dilation	Ducharme et al., 2000
MMP-9 knockout in mice with ischemia/reperfusion injury	Protected against ischemia- induced myocardial injury	Romanic et al., 2002
TIMP-1 knockout in mice	Reduced myocardial fibrillar collagen content; Increased end-diastolic wall stress; Unchanged systolic pressure and ejection performance; No distinctive myocardial phenotype under unstressed stage	Roten et al., 2000

Continued

Experimental model	Key findings	Reference
TIMP-1 knockout in mice with MI	Amplified adverse LV remodeling after MI	Creemers et al., 2003
TIMP-1 knockout in mice with MI	Accelerated myocardial remodeling induced by TIMP-1 gene deletion can be pharmacologically rescued by MMP inhibition	Ikonomidis et al., 2005
TIMP-3 knockout in mice	Interstitial matrix disruption with elevated MMP-9 activity; Activation of tumor necrosis factor-α; LV dilation and dysfunction with age	Fedak et al., 2004
MMP-1 overexpression in mice	Myocyte hypertrophy, increased cardiac collagen at 6 months of age; Systolic and diastolic dysfunction at 12 months of age	Kim et al., 2000
MMP-2 overexpression in mice	Severe LV contractile dysfunction with age; Increased interstitial and perivascular fibrosis	Bergman et al., 2007
TIMP-1 overexpression in mice with MI	Preserved cardiac function and ventricular geometry; Reduction in myocardial fibrosis and MMP activity	Jayasankar et al., 2004
TIMP-4 cardiac-specific overexpression	Decreased heart/body weight ratio; increased fibrosis and apoptosis, diastolic dysfunction	Kassiri and Khokha, 2005

LV, left ventricle; MI, myocardial infarction

Table 3. Classification and nomenclature of the MMPs

MMPs	Alternative name	Substrates
MMP-1	Collagenase (Type I, interstitial)	Collagens (I, II, III, VII, VIII, and X); gelatin; aggrecan; L-selectin; IL-1beta; proteoglycans; entactin; ovostatin; MMP-2; MMP-9
MMP-2	Gelatinase A 72 kDa Gelatinase Type IV Collagenase	Collagens (I, IV, V, VII, and X); gelatin; entactin; aggrecan; gelatin; fibronectin; osteonectin; plasminogen; MBP; TNF precursor, pro-TGF-beta
MMP-3	Stromelysin-1, Proteoglycanase	Collagens (III, IV, V, and IX); gelatin; aggrecan; perlecan; decorin; laminin; elastin; caesin; osteonectin; ovostatin; entactin; plasminogen; MBP; IL-1beta; MMP-2/TIMP-2; MMP-7; MMP-8; MMP-9; MMP-13
MMP-7	Matrilysin; PUMP	fibronectin; laminin; entactin; elastin; casein; transferrin; plasminogen; MBP; Beta4-intergrin; MMP-1; MMP-2; MMP-9; MMP-9/TIMP-1
MMP-8	Neutrophil collagenase	Collagens (I, II, III, V, VII, VIII, and X); gelatin; aggrecan; fibronectin
MMP-9	Gelatinase B	Collagens (IV, V, VII, X, and XIV); gelatin; entactin; aggrecan; elastin; fibronectin; osteonectin; plasminogen; MBP; IL-1beta
MMP-10	Stromelysin-2	Collagens (III-V); gelatin; casein; aggrecan; elastin; MMP-1; MMP-8
MMP-11	Stromelysin-3	IGFBP; α1PI
MMP-12	Macrophage metalloelastase	Collagen IV; gelatin; elastin; casein; fibronectin; vitronectin; laminin; entactin; MBP; fibrinogen; fibrin; plasminogen
MMP-13	Collagenase-3	Collagens (I, II, III, IV, IX, X, and XIV); gelatin; plasminogen;aggrecan; perlecan; fibronectin; osteonectin; MMP-9
MMP-14	MT1-MMP	Collagens (I-III); gelatin; casein; fibronectin; laminin; vitronectin; entactin; proteoglycans; MMP-2; MMP-13

Continued

MMPs	Alternative name	Substrates
MMP-15	MT2-MMP	Fibronectin; entactin; laminin; aggrecan; perlecan; MMP-2
MMP-16	MT3-MMP	Collagen III; gelatin; casein; fibronectin; MMP-2
MMP-17	MT4-MMP	Gelatin; TNF-α precursor; fibrillin; gibronectin
MMP-18	Xenopus Collagenase-4	Type I collagen
MMP-19	RASI	Type I collagen
MMP-20	Enamelysin	Amelogenin; aggrecan, and cartilage oligomeric matrix protein (COMP)
MMP-21	Xenopus MMP (X-MMP)	Unknown
MMP-22	Chicken MMP (C-MMP)	Unknown
MMP-23	Cysteine Array Matrix Metalloproteinase (CA-MMP)	Gelatin
MMP-24	MT5-MMP	Fibronectin, but not collagen type I nor laminin
MMP-25	MT6-MMP; leukolysin	Pro-gelatinase A
MMP-26	Matrilysin-2; Endometase	Collagen IV, fibronectin, fibrinogen, gelatin, alpha (1)-proteinase inhibitor
MMP-27		Unknown
MMP-28	Epilysin	Casein

(Hijova, 2005)

Table 4. Characteristics of TIMPs

	TIMP-1	TIMP-2	TIMP-3	TIMP-4
Protein kDa	28	21	24/27	22
N-glycosylation sites	2	0	1	0
Protein localization	Soluble	Soluble/cell surface	ECM	Soluble/cell surface
Pro-MMP association	pro-MMP-9	pro-MMP-2	pro-MMP-2/-9	pro-MMP-2
MMPs poorly inhibited	MT1-MMP MT2-MMP MT3-MMP MT5-MMP MMP-19	None	None	None
ADAM inhibition	ADAM 10	None	ADAM 12 ADAM 17 ADAM 19 (ADAM 10) ADAMTS-4, TS-5	None
Cell proliferation	Erythroid precursors Tumour cells	Erythroid precursors Tumour cells Fibroblasts Smooth muscle cells Endothelial cells	Smooth muscle cells and cancer cells	Mammary tumour cells Wilm's tumour cells
Apoptosis	Burkitt's lymphoma cells	Colorectal cancer cells Melanoma	Smooth muscle cells Tumour cells Retinal pigmented epithelial cells	Cardiac fibroblasts
Tumour angiogenesis	Mammary Liver	Melanoma Mammary	Melanoma	
Angiogenesis in 3D collagen/fibrin gels	No effect	Inhibits	Inhibits	Inhibits
Tumourigenesis effects	Inhibits	Inhibits	Inhibits	Inhibits
Metastasis effects	Stimulates			Stimulates

MT-MMP, membrane-type matrix metalloproteinase; ADAM, a disintegrin and metalloproteinase; ADAMTS, a disintegrin and metalloproteinase thrombospondin type (Baker et al., 2002)

Table 5. Primers used in this study for Semi-quantitative RT-PCR and Real-time PCR

Genes	Accession no.	Forward primers (5' → 3') Reverse primers (5' → 3')	Product size (bp)
Semi-quantitative RT-PCR			
GAPDH	NM_008084	GGTGATGCTGGTGCTGAGTA TTCAGCTCTGGGATGACCTT	413
ANP	NM_008725	CTGCTAGACCACCTGGAGGAG CAGGAGGGTGTTCACCACGC	455
BNP	NM_008726	AAGCTGCTGGAGCTGATAAGA GTTACAGCCCAAACGACTGAC	222
Col1a2	NM_007743	AGACCCAAGGACTATGAAGT ATGCTGTTCTTGCAGTGGTA	446
Col3a1	NM_009930	CTGCAAGATGGATGCTA CATCAGCTTCAGAGACT	328
TIMP-1	NM_001044384	TCTGGCATCCTCTTGTTGCT CACAGCCAGCACTATAGGTCTTT	418
TIMP-2	NM_011594	GTAGTGATCAGAGCCAAAG TTCTCTGTGACCCAGTCCAT	416
TIMP-3	NM_011595	TCTGCAACTCCGACATCGTG CGGATGCAGGCGTAGTGTT	454
TIMP-4	NM_080639	TCCGGTATGAAATCAAACAGAT GTGATTTGGCAGCCACAGTT	271
Real-time PCR			
GAPDH	NM_008084	AGGTTGTCTCCTGCGACTTCA CCAGGAAATGAGCTTGACAAAGTTGTC	101
MMP-2	NM_008610	CCCCATGAAGCCTTGTTTACCATG TTGTAGGAGGTGCCCTGGAAG	86
MMP-9	NM_013599	AGACCAAGGGTACAGCCTGTTC GGCACGCTGGAATGATCTAAGC	78

GAPDH, glyceraldehyde-3-phosphate dehydrogenase; ANP, natriuretic peptide precursor type A; BNP, natriuretic peptide precursor type B; Col1a2, collagen type I alpha2; Col3a1, collagen type III alpha1

Table 6. Changes in the ventricular weight and tail length of mice with doxorubicin treatment

	Week 1		Week 3		Week 5		Week 9		Week 12	
	Ct (n=5)	Dox (n=10)	Ct (n=5)	Dox (n=9)	Ct (n=5)	Dox (n=10)	Ct (n=3)	Dox (n=8)	Ct (n=4)	Dox (n=10)
Ventricular weight (mg)	110 ± 3	110 ± 7	127 ± 10	89 ± 6[a]	118 ± 7	93 ± 6[a]	131 ± 9	88 ± 9[a]	119 ± 2	83 ± 8[a]
Tail length (cm)	7.9 ± 0.1	8.0 ± 0.1	8.2 ± 0.2	7.5 ± 0.0[a]	7.9 ± 0.1	8.0 ± 0.2	8.1 ± 0.6	8.0 ± 0.0	8.1 ± 0.2	8.0 ± 0.1
Ventricular weight/tail length ratio (mg/cm)	13.9 ±0.4	13.8 ±1.0	15.6 ±1.4	11.9 ±0.8[a]	14.9 ±0.9	11.7 ±0.7[a]	16.1 ±1.1	11.0 ±1.1[a]	14.7±0.1	10.4 ±0.8[a]

Ct and Dox indicate the group of sham control and doxorubicin, respectively. [a] indicate $P < 0.01$ compared with the sham control within each group.

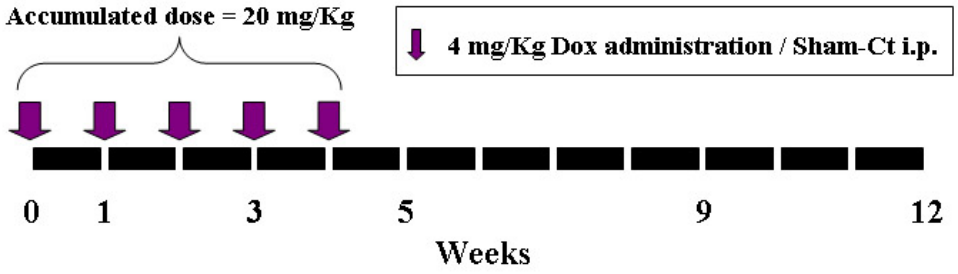

Figure 1. Experimental protocol. The mice were administered 4 mg/kg i.p. of doxorubicin hydrochloride (Dox), in a concentration of 1 mg/mL, five times weekly to reach accumulated dosage of 20 mg/kg. Injection of equivalent volume of saline was as sham control. The hearts of the mice were harvested at week 1, 3, 5, 9, and 12 after the first injection.

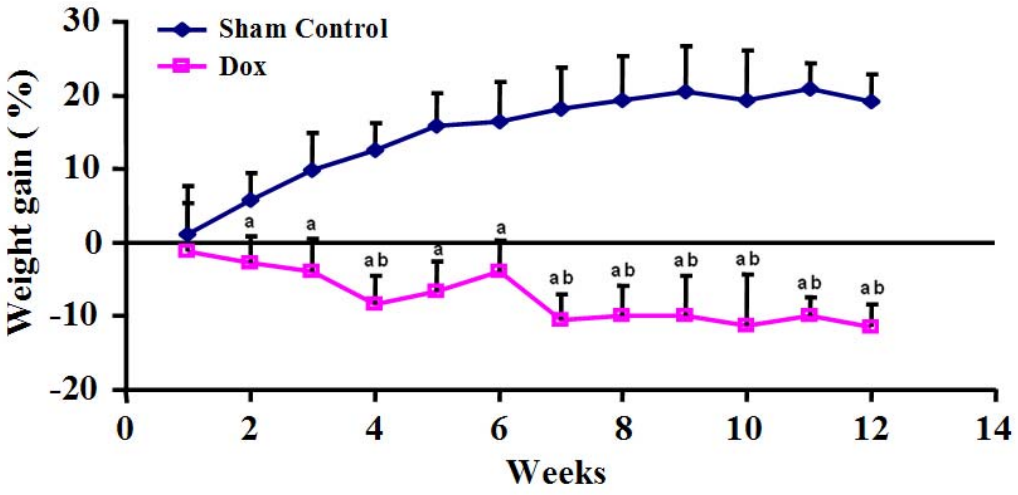

Figure 2. Percentage of weight change of the animals. Body weight of mice dropped obviously with Dox treatment. Without recovery even the administration had been stopped. Data represent mean ± SD. [a] indicate $P < 0.01$ relative to time-matched sham control, and [b] indicate $P < 0.01$ relative to the beginning in the group with Dox treatment.

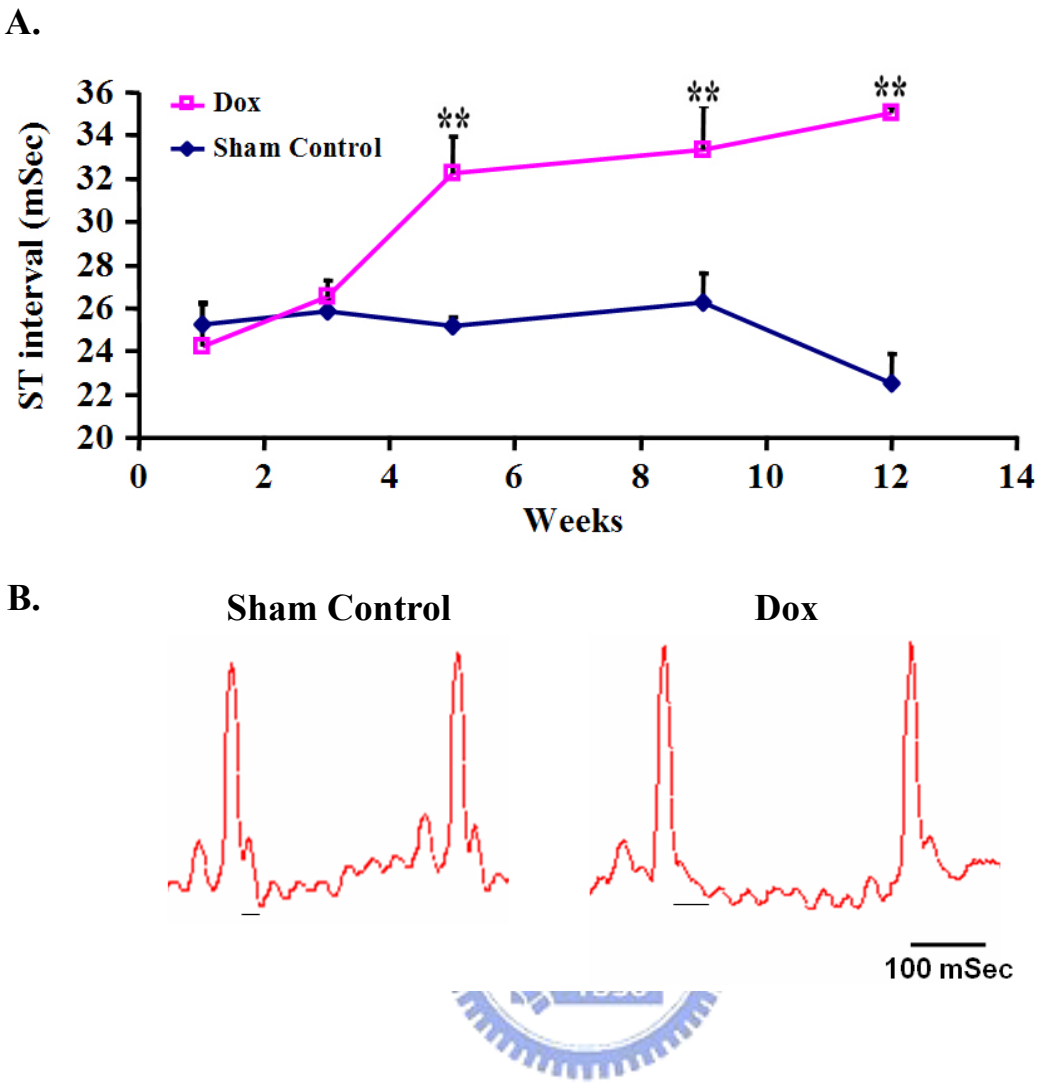

Figure 3. ST-interval prolongation after Dox treatment. It was measured with the use of lead II ECG under anesthesia. The ST interval in Dox-treated group increased with time **(A)**. Typical ECG trace recorded for mice in control and Dox treatment **(B)**. In the ECG, the ST interval is indicated by the bar. Data represent mean ± SD. ** indicate $P < 0.01$ relative to the control.

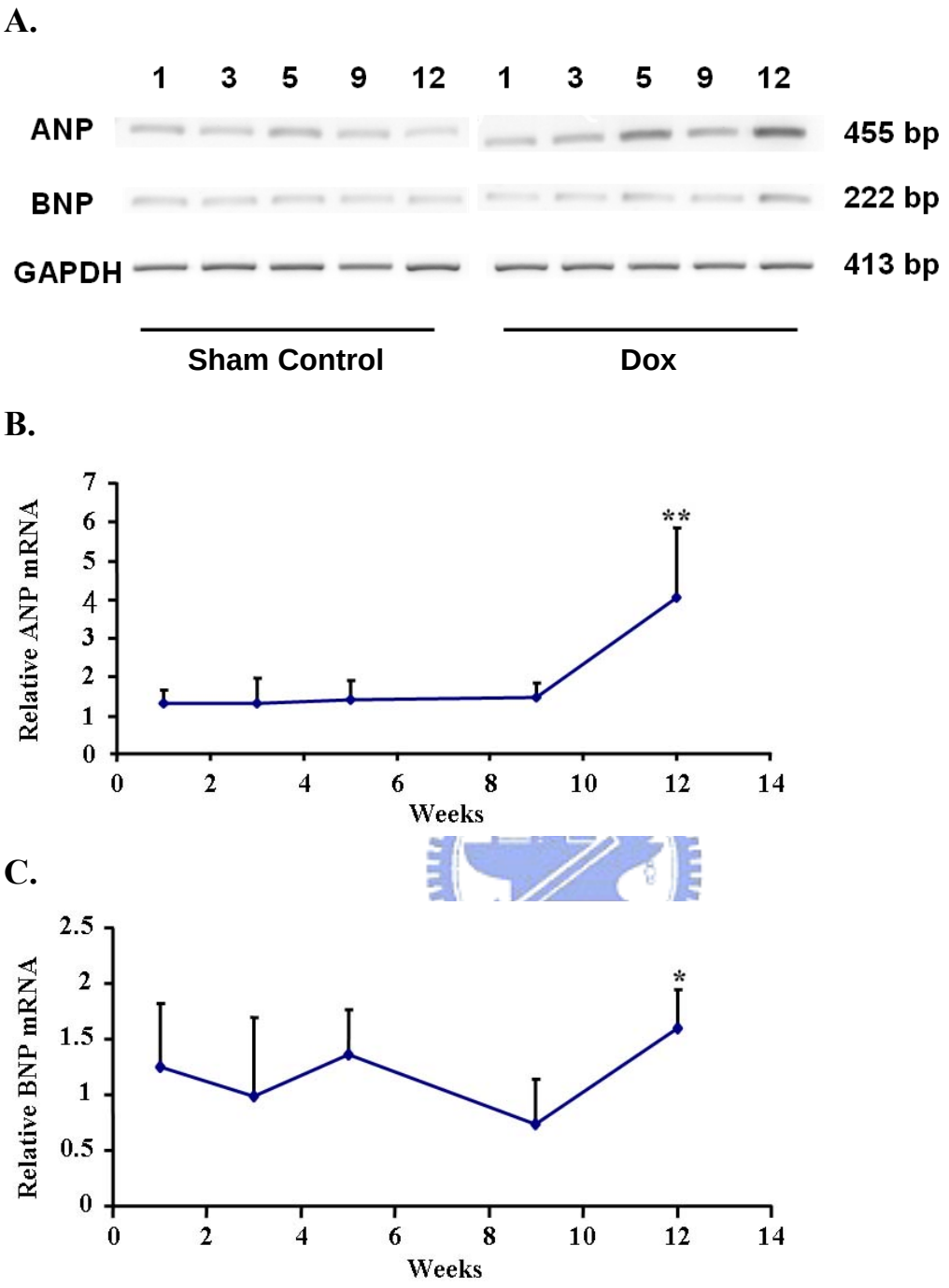

Figure 4. Induction of ANP and BNP mRNA in the LV with Dox treatment. The cDNAs prepared from LV were subjected to PCR **(A)**. The mRNA expression level of ANP **(B)** and BNP **(C)** was presented as fold relative to time-matched sham control. GAPDH was used as internal control. Data represent mean ± SD. * and ** indicate $P < 0.05$ and $P < 0.01$ relative to the control, respectively.

A. Sham Control

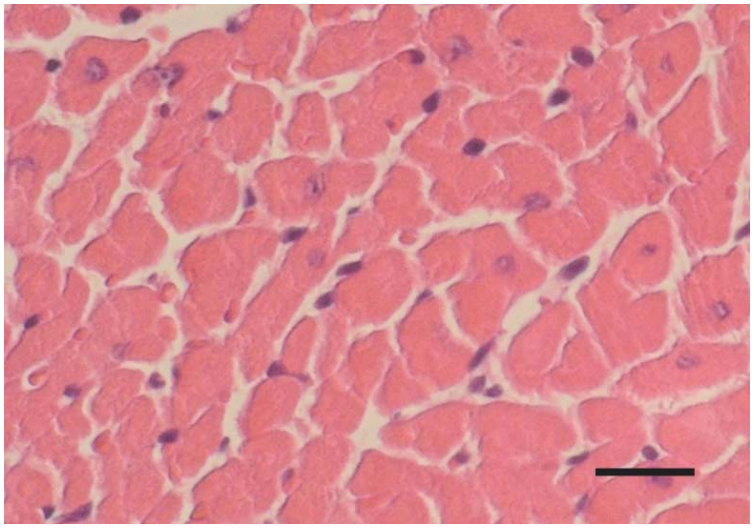

B. Dox

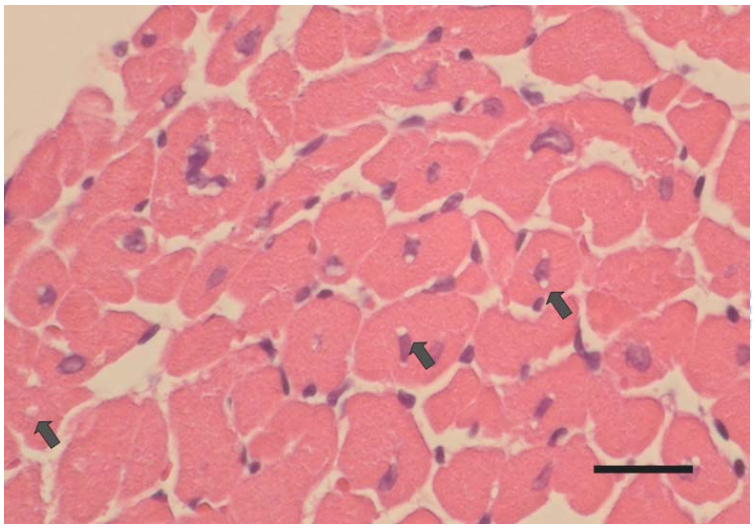

Figure 5. HE stain of the ventricles from the mice in Dox and sham control group. Hearts were examined at week 12 by using of hematoxylin and eosin staining. Comparing with control **(A)**, hearts of Dox-treated mice **(B)** showed vacuole formation (arrow). (Scale bars represent 25 μm.)

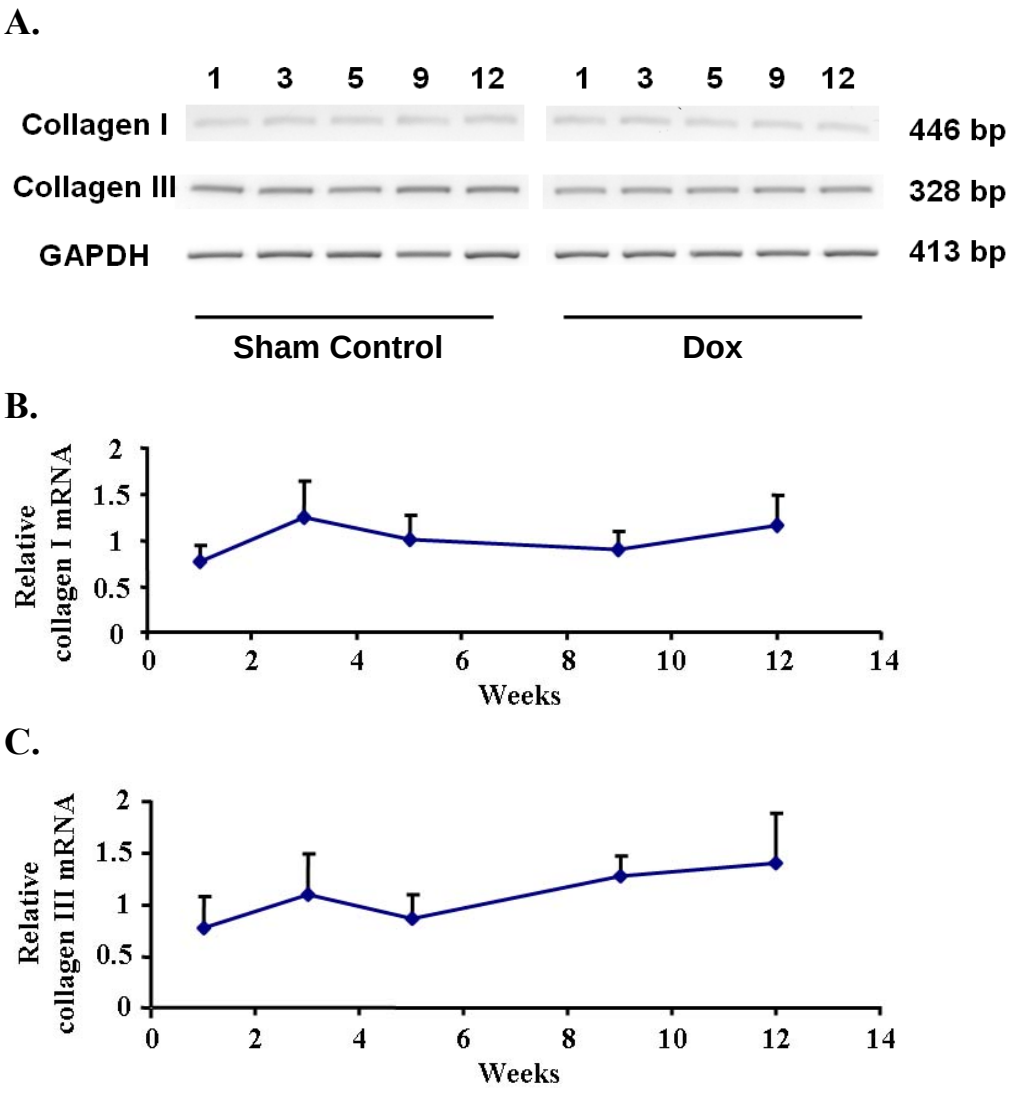

Figure 6. The mRNA expression of collagen type I and III in LV. The cDNAs prepared from LV were subjected to PCR **(A)**. The expression level of collagen Ia2 **(B)** and collagen IIIa1 **(C)** was presented as fold relative to time-matched sham control. GAPDH was used as internal control. Data represent mean ± SD.

A.

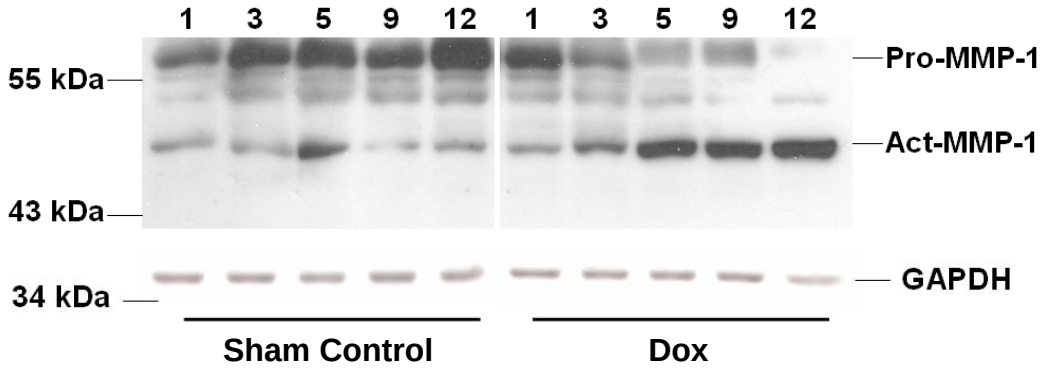
1 3 5 9 12 1 3 5 9 12
55 kDa
43 kDa
34 kDa
Pro-MMP-1
Act-MMP-1
GAPDH
Sham Control
Dox

B.

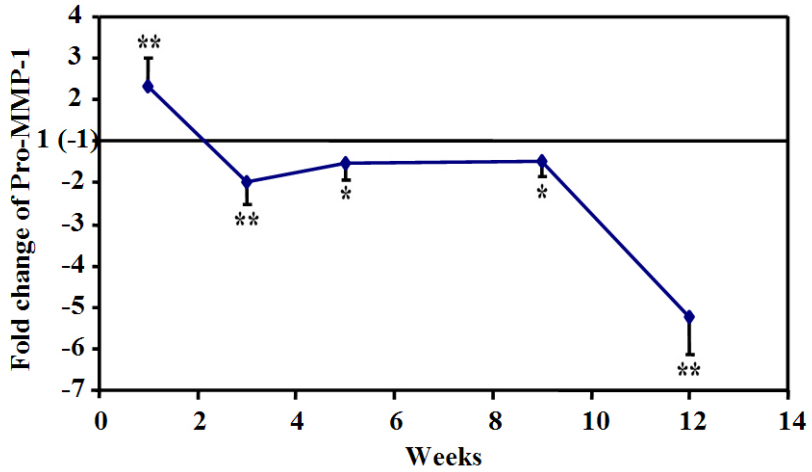
Fold change of Pro-MMP-1
Weeks
4
3
2
1 (-1)
-2
-3
-4
-5
-6
-7
0 2 4 6 8 10 12 14
**
**
*
*
**

C.

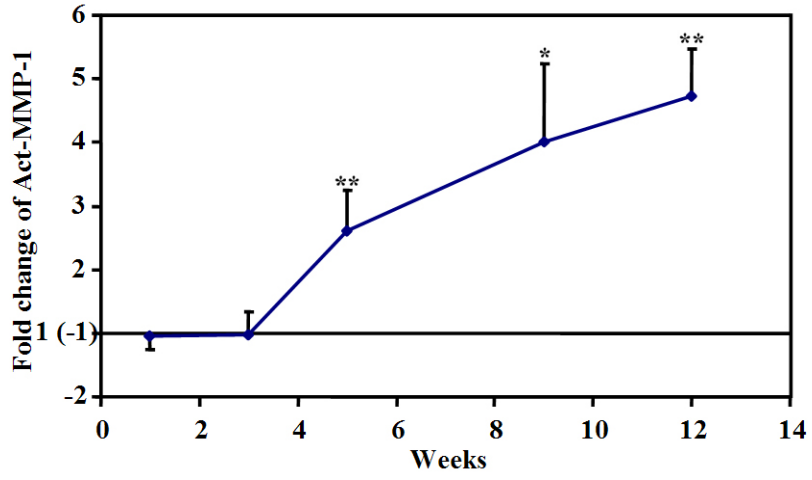
Fold change of Act-MMP-1
Weeks
6
5
4
3
2
1 (-1)
-2
0 2 4 6 8 10 12 14
**
*
**

D.

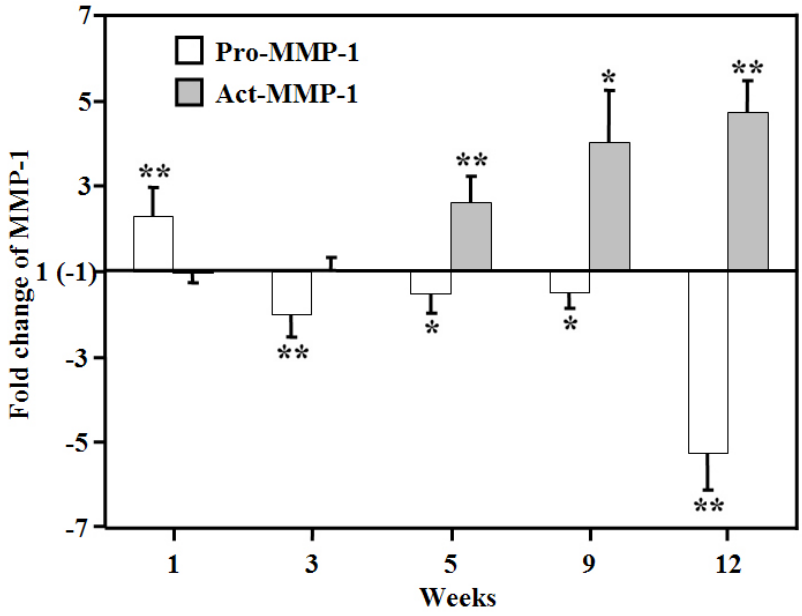

E.

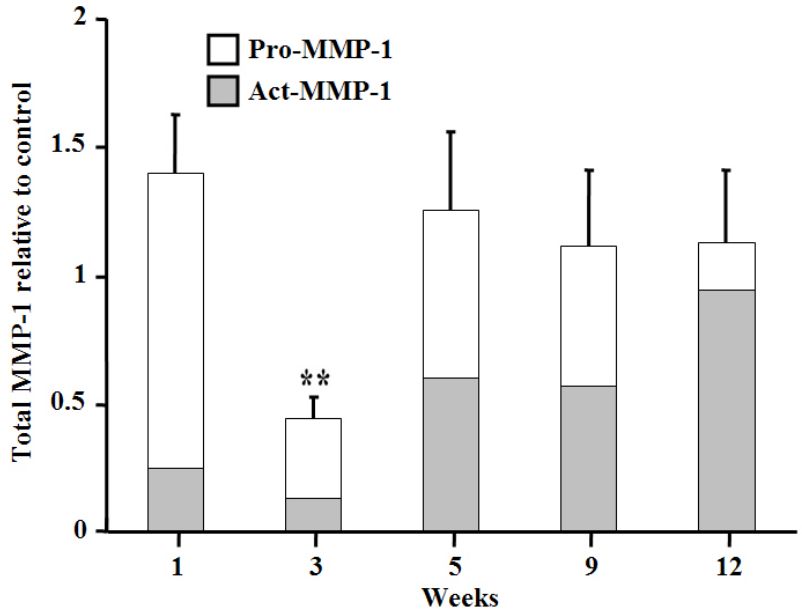

Figure 7. Opposite trends of changes in latent and active MMP-1. The 57 kDa glycosylated latent pro-MMP-1 and 47 kDa active MMP-1 were detected on membrane by immunoblotting, GAPDH was used as internal control **(A)**. The decrease on pro-MMP-1 **(B)** and increase on act-MMP-1 **(C)** over time were expressed as a relative fold change standardized to time-matched sham control group. The combination illustrates an opposite pattern **(D)** with unchanged protein level of total MMP-1 **(E)**. Data represent mean ± SD. * and ** indicate $P < 0.05$ and $P < 0.01$ relative to the control, respectively.

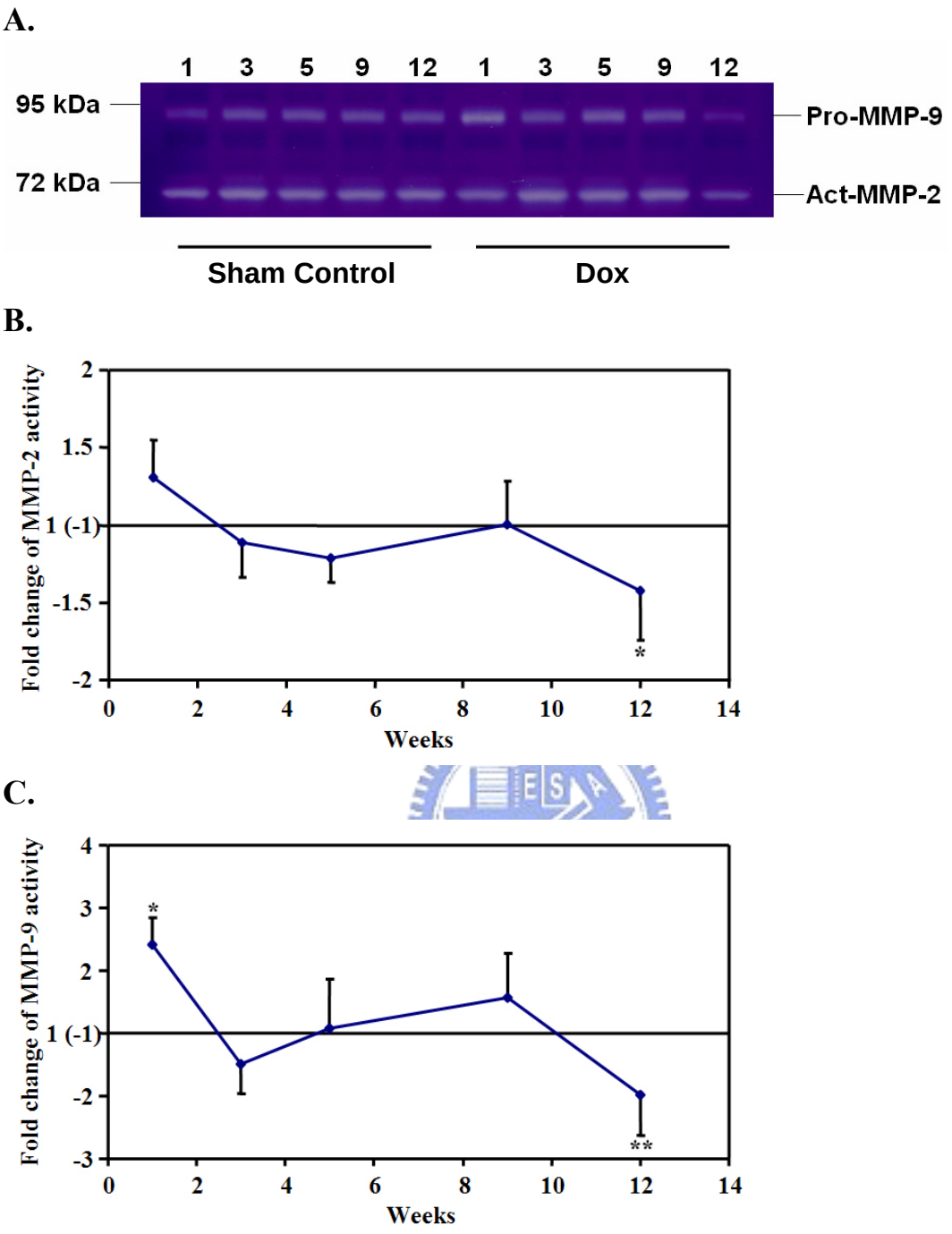

Figure 8. Reduction of gelatinases activity in the LV with Dox treatment. Gelatinolytic activity of MMP-2 and MMP-9 (92 kDa) in LV tissues were determined by zymographic analysis (20 μg per each determination) **(A)**. The 72 kDa pro-form and the 68 kDa activation intermediate form of MMP-2 were indicated. This intermediate form of MMP-2 had a 1.5 fold slight decrease on week 12 compared with control (*, $p < 0.05$ relative to the control**) (B)**. The reduction of MMP-9 activity in Dox group during week 12 reached statistical significance (**, $p < 0.01$ relative to the control) **(C)**. However, there were insignificantly different between the two groups on the 72 kDa pro-MMP-2. The quantity was expressed as a relative fold change relative to time-matched sham control group.

A.

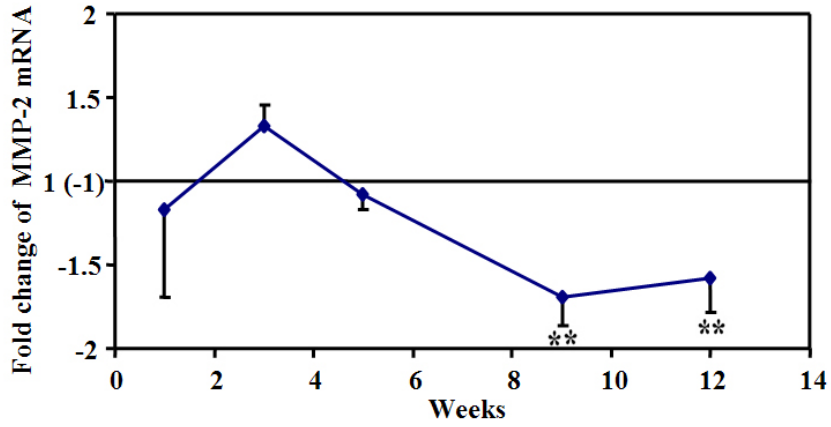

B.

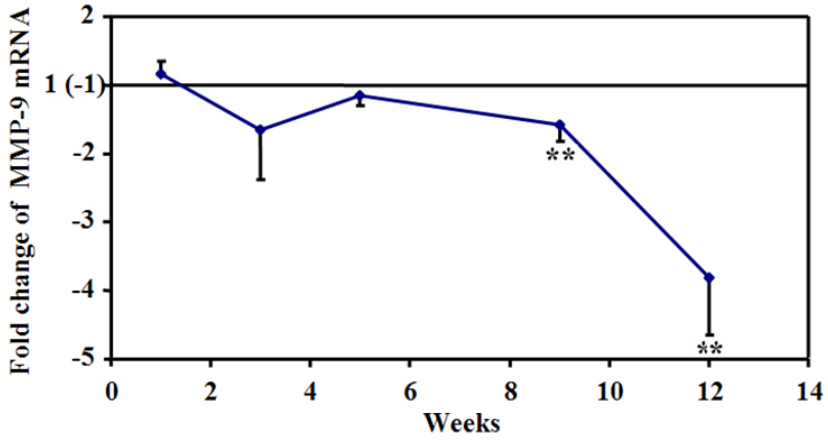

Figure 9. Decreased mRNA expression of gelatinases in the LV with Dox treatment. Comparisons of mRNA expression in the LV, the cDNAs were prepared from the LV of two groups and then subjected to real-time PCR with gene-specific primers. The ratio of the abundance of MMP transcript to that of the GAPDH transcript was calculated, and the amount of MMP-2 **(A)** and MMP-9 **(B)** mRNA expression in the Dox group was expressed as a relative change standardized to time-matched sham control group. Data represent mean ± SD. ** indicate $P < 0.01$ relative to the control.

A.

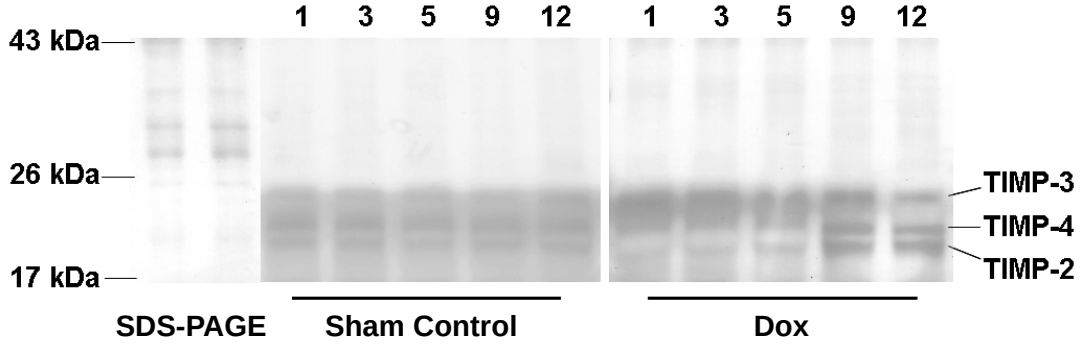
1 3 5 9 12 1 3 5 9 12
43 kDa
26 kDa
17 kDa
TIMP-3
TIMP-4
TIMP-2
SDS-PAGE
Sham Control
Dox

B.

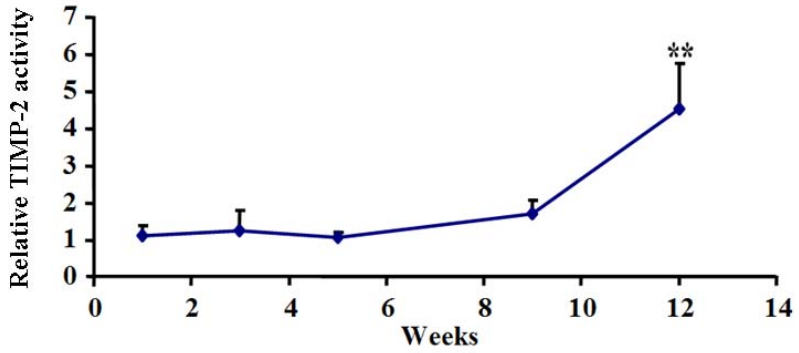
Relative TIMP-2 activity
0 1 2 3 4 5 6 7
0 2 4 6 8 10 12 14
Weeks
**

C.

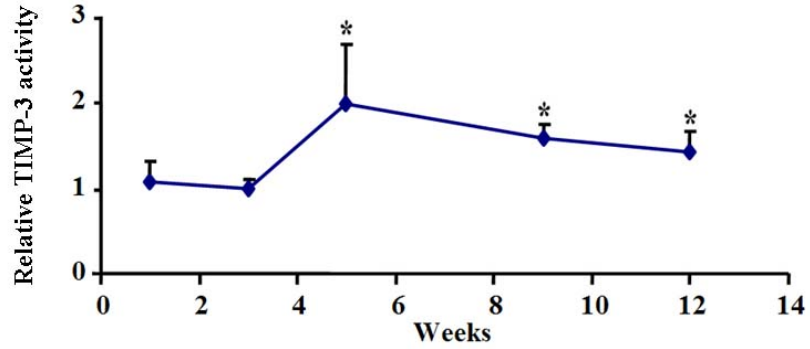
Relative TIMP-3 activity
0 1 2 3
0 2 4 6 8 10 12 14
Weeks
*
*
*

D.

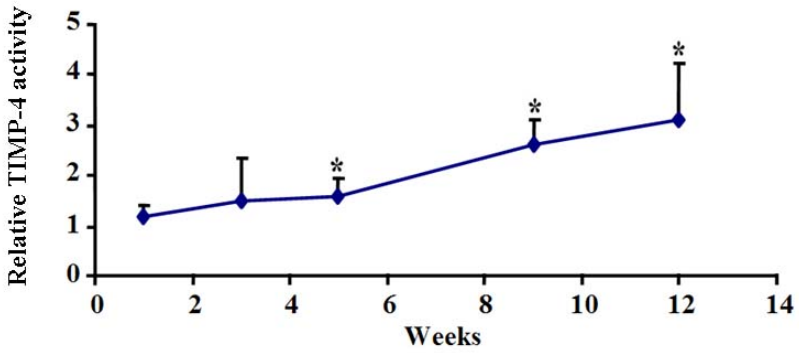

Figure 10. Up-regulation of TIMPs activity by reverse zymography in Dox-treated mice. Inhibitory activity of TIMPs was analyzed by reverse zymography as described in materials and methods. Dark bands were undigested gelatin stained with Coomassie blue, representing areas of MMP inhibition. The TIMP-2, -3 and -4 were identified upon molecule weight as 21, 24 and 22 kDa, respectively. The bands from total protein and inhibitory activity of TIMPs were distinguished by comparing with SDS-PAGE **(A)**. The increased activity of TIMPs with Dox treatment was illustrated **(B~D)** as fold relative to time-matched sham control. Data represent mean ± SD. * and ** indicate $P < 0.05$ and $P < 0.01$ relative to the control, respectively.

A.

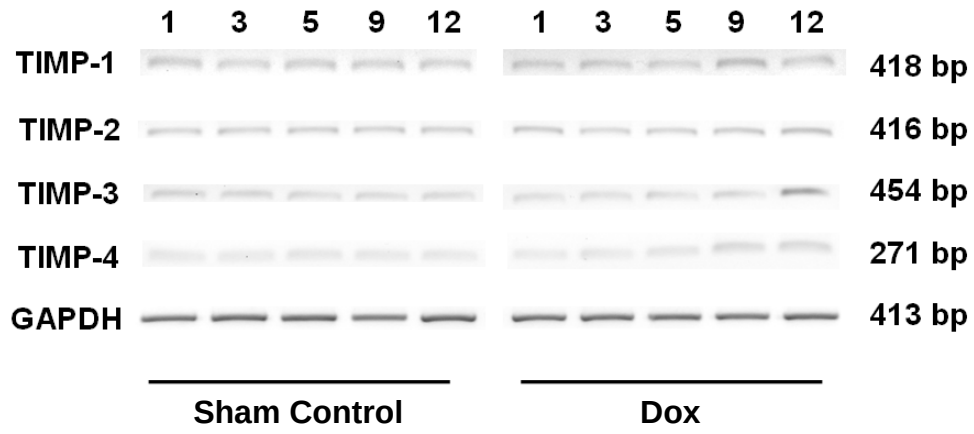
1 3 5 9 12 1 3 5 9 12
TIMP-1
TIMP-2
TIMP-3
TIMP-4
GAPDH
418 bp
416 bp
454 bp
271 bp
413 bp
Sham Control
Dox

B.

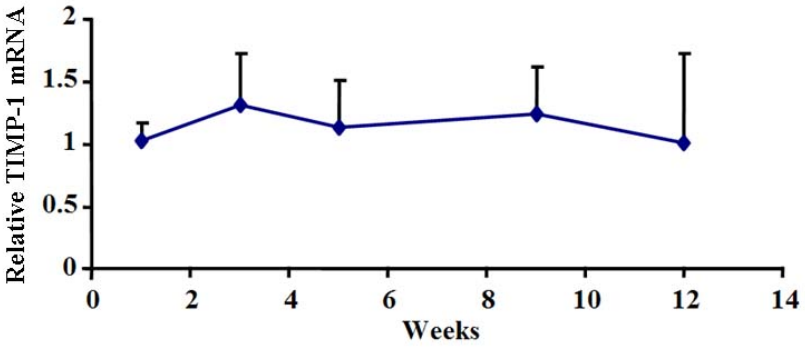
Relative TIMP-1 mRNA
2
1.5
1
0.5
0
0 2 4 6 8 10 12 14
Weeks

C.

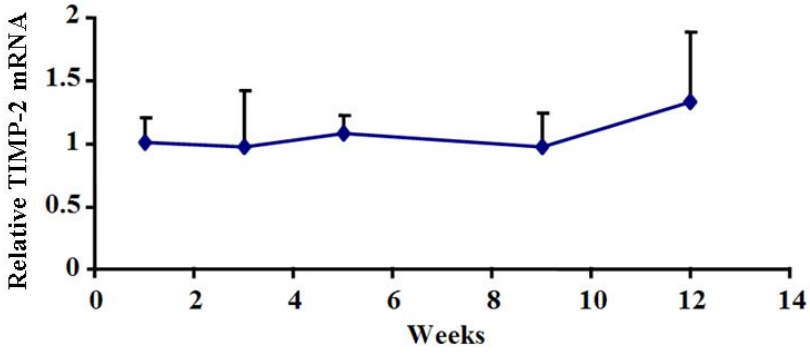
Relative TIMP-2 mRNA
2
1.5
1
0.5
0
0 2 4 6 8 10 12 14
Weeks

D.

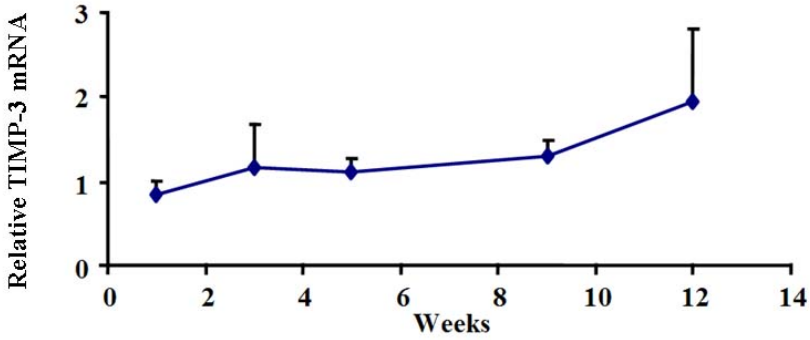

E.

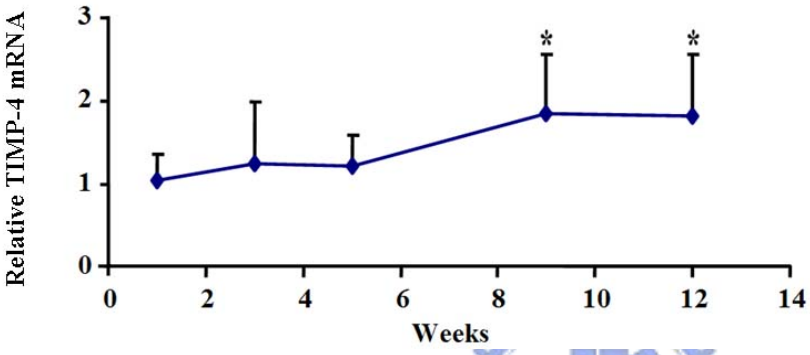

Figure 11. The mRNA expression of TIMPs in the LV with Dox treatment. The cDNAs prepared from LV were subjected to PCR **(A)**. Except the slight increase on TIMP-4 mRNA **(E)**, no significant differences were observed between Dox and control groups **(B~D)**. The expression level was presented as fold relative to time-matched sham control. GAPDH was used as internal control. Data represent mean ± SD. * indicate $P < 0.05$ relative to the control**.**

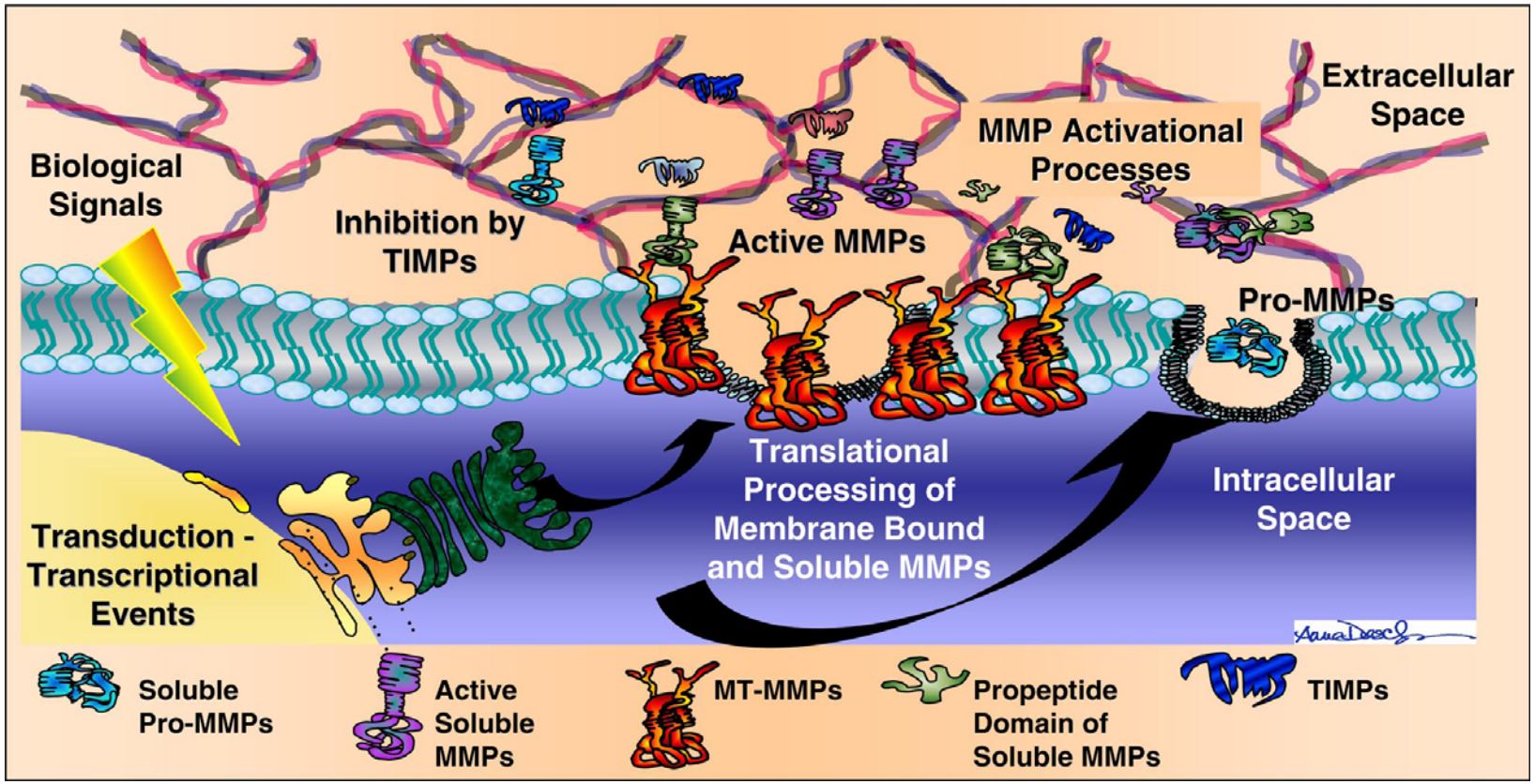

Appendix-I. A simplified schematic of the current concepts regarding the regulation of MMP activity within the myocardial interstitium. MMPs and TIMPs are regulated on various levels including transcriptional, posttranscriptional and posttranslational steps. After secretion, the activation of the latent MMPs requires proteolytic cleavage of the prodomain, which can occur by other proteases or by the MT-MMPs. This MMP activation step provides for focal proteolytic activity but can quickly amplify as additional MT-MMPs or soluble MMPs are synthesized. Additionally, the active MMPs (both MT-MMPs and soluble MMPs) are inhibited by the TIMPs. (Spinale, 2007)

A.

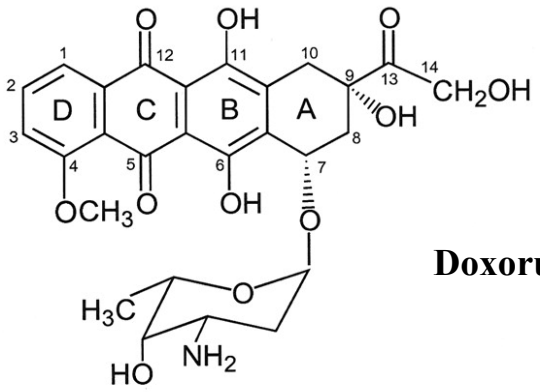

Doxorubicin

B.

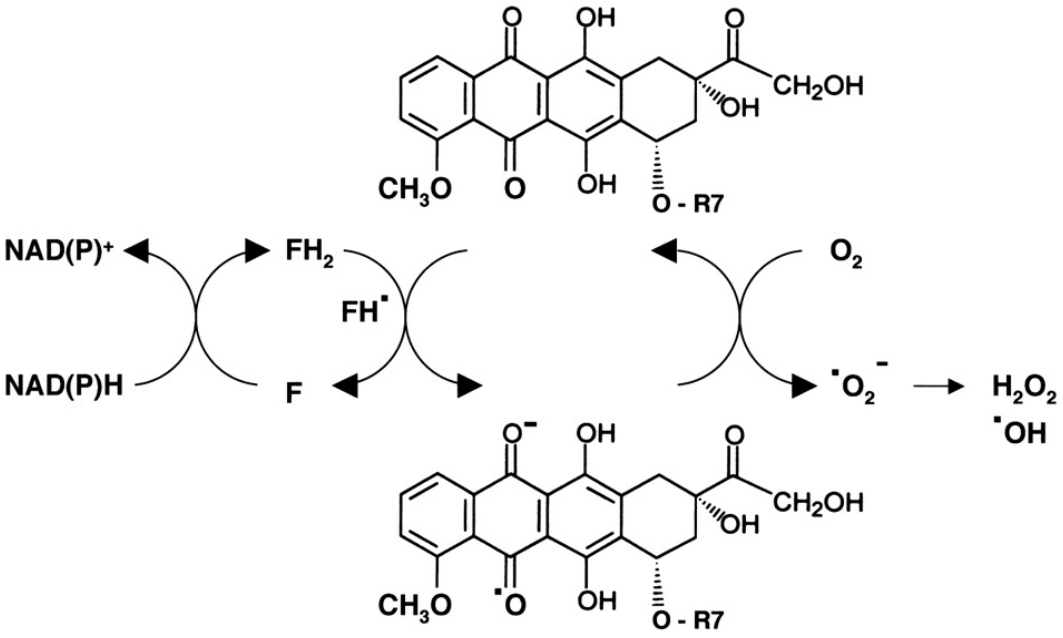

Appendix-II. The structure and redox cycle of doxorubicin. Structure of doxorubicin **(A)**. The quinone ring undergoes redox cycling between quinone and semiquinone states. During this process, electrons generated are captured by oxidizing agents, including oxygen, which then initiate a chain reaction leading to the generation of reactive oxygen species **(B)**. (Minotti et al., 2004; Takemura and Fujiwara, 2007)